Characterization of the Ubiquitin Kinase Activity of PINK1

by

Shafqat Rasool

McGill University, Montreal

December, 2015

A THESIS SUBMITTED TO MCGILL UNIVERSITY IN PARTIAL OF THE REQUIREMENTS OF THE DEGREE OF

MASTER OF SCIENCE

Biochemistry (Thesis)

In

Faculty of Medicine

Table of Contents

Abstract

Mutations in the PINK1- and Parkin-encoding genes cause autosomal recessive form of Parkinson's disease. PINK1 is a protein kinase, best known for its role in signaling mitochondrial damage and consequently initiating mitochondrial repair or autophagy mechanisms. Upon mitochondrial damage, PINK1 accumulates on the outer membrane (OMM) of the mitochondria, and recruits the E3 ubiquitin ligase Parkin in a kinase activity-dependent fashion. Parkin then ubiquitinates multiple OMM proteins and signals mitochondria for autophagic destruction. In recent years, the mechanism for Parkin's recruitment and activation has been a subject of extensive study in the context of PINK1's kinase activity. The most recent evidence suggests that the role of PINK1 is to phosphorylate both Parkin (on its ubiquitin-like domain) and ubiquitin on Ser65 for a complete activation of Parkin. This makes PINK1 the first known ubiquitin kinase. However the underlying molecular mechanisms underlying Parkin's activation are unknown. Here, I have developed a PINK1 production system to characterize the kinetics of Parkin and ubiquitin phosphorylation and its consequences for the activation of Parkin. After optimization, I found that the PINK1 ortholog from the insect species *Tribolium castaneum* (TcPINK1) expresses well in E. coli, can be purified in solution, and produces an active kinase. This recombinant PINK1 was essential to elucidate the role of phosphorylated ubiquitin (pUb) as an enhancer for Parkin phosphorylation by PINK1, hence establishing a role of pUb in the mitochondrial quality control pathway. Nuclear magnetic resonance studies and phosphorylation assays combined with mutagenesis reveal the residues in Parkin that are critical for the interactions with PINK1. This work sets the stage for more detailed investigations of the structural features of PINK1 that allow the enzyme to recognize ubiquitin domains and phosphorylate specifically Ser65.

Résumé

Des mutations dans les gènes codant PINK1 et Parkin causent une forme récessive autosomale de la maladie de Parkinson. PINK1 est une kinase de protéine, bien connu pour son rôle dans la signalisation de dommages mitochondriaux et conséquemment l'initiation de mécanismes de réparations par autophagie. PINK1 s'accumule sur la membrane externe des mitochondries (MEM) endommagées, et ensuite recrute la ligase d'ubiquitine Parkin via son activité kinase. Dès lors, Parkin ubiquitine de nombreuses protéines de la MEM, ce qui entraine la destruction autophagique de ces mitochondries. Au cours des cinq dernières années, les mécanismes de recrutement et d'activation de Parkin dans le contexte de l'activité kinase de PINK1 furent l'objet de plusieurs études. Ces études ont convergées sur un modèle où PINK1 phosphoryle Parkin (dans son domaine similaire à l'ubiquitine) et l'ubiquitine sur Ser65, résultant dans l'activation complète de Parkin. Ceci fait donc de PINK1 la première kinase d'ubiquitine connue. Hors, les mécanismes moléculaires de l'activation de Parkin reste énigmatiques. Dans cette thèse, j'ai développé un système de production de PINK1 pour caractériser la cinétique de phosphorylation de Parkin et de l'ubiquitine, ainsi que pour déterminer les conséquences sur l'activation de Parkin. Après optimisation, j'ai découvert que l'orthologue de PINK1 dérivée de l'insecte *Tribolium castaneum* (TcPINK1) exprime bien dans E. coli, se purifie en solution, et produit une kinase active. Cette PINK1 recombinante fut essentielle afin d'élucider le rôle de l'ubiquitine phosphorylée (pUb) dans la stimulation de la phosphorylation de Parkin par PINK1, établissant donc le rôle de pUb dans la voie de contrôle de qualité des mitochondries. Des expériences de résonance magnétique nucléaire et des essais de phosphorylation couplés à de la mutagénèse ont révélés les acides aminés dans Parkin qui sont essentielles pour son interaction avec PINK1. Ces travaux préparent le terrain pour des études plus approfondies sur les attributs structuraux de PINK1 qui lui permettent de reconnaitre le domaine ubiquitine et de phosphoryler spécifiquement la Ser65.

Acknowledgements

I would like to thank my supervisor Dr. Jean-Francois Trempe for accepting me in his lab as a graduate student. Being the first member of the Trempe lab is something that I am both extremely honored and excited about. The work presented in this thesis owes itself in no small measures to the encouragement that I received from him, and from the confidence I gained by discussing science with him. I would like to thank my co-supervisor Dr. Kalle Gehring for allowing me to affiliate with him. The academic guidance and research directions that he has provided me with has ensured that I continue to make progress in my project. Working with Dr. Gehring also allowed me to familiarize with various cutting-edge structural biology techniques.

I would like to thank Nathalie Croteau for the technical assistance, and for sharing resources and information that were key to the development of the project, and Dr. Marta Vranas for fruitful discussions on literature relevant to the project. I would like to thank all other members of the Trempe lab as well for making the time spent at lab absolutely worthwhile. From Gehring lab, I would like to give thanks to Veronique Sauvé for sharing the human PINK1 constructs and giving valuable technical advice. I would also like to thank Dr. Marie Menade and Dr. Maxim Isabelle for their technical support.

I would like thanks members of my research advisory committee, Dr. Martin Scheming and Dr. Simon Wing, for providing important feedback on my research and presentation skills. I am grateful of Dr. Lisa Munter (Pharmacology, McGill) for assistance with MALDI-TOF mass spectrometry. I would also like to thank Noriyuki Matsuda (Tokyo) for providing the plasmids for His-Ub and His-UbS65A. Funding from Bionano (NSERC-CREATE training program) throughout my master's program was very helpful for me and my project.

Lastly, just like every other thing in my life, I would like to thank my mother for raising me and providing for me in a way that allowed my attendance at McGill University; the dreams that have come true and are yet to come true were conceived in her warm embrace.

Author Contributions

I performed all the experiments in reported in this thesis with the exception of the following:

Small - scale expression testing of PINK1 orthologs (Figure 3.5) was performed my Nathalie Croteau. ITC experiments (Figure 5.1 B) and sample preparation for SAXS (Figure 5.1 C) were performed by Veronique Sauvé. Pairwise-distance distributions and R_g calculations (Figure 5.1 C) based on SAXS were performed by Jean-Francois Trempe. NMR experiment for ^{15}N-Ubl with R0RBR and/or pUb were performed by Marjan Seirafi. His-Ub diagnostic phosphorylation assay was performed with Jean-Francois Trempe (Figure 4.1 A) and MALDI-TOF analysis was performed with Lisa Munter.

The experiments were conceived by Jean-Francois Trempe.

List of Abbreviations

AMP-PNP	Adenylyl-imidophosphate
ATP	Adenosine triphosphate
CCCP	Carbonyl cyanide m-cholorphenyl hydrazone
EGFR	Epidermal growth factor receptor
HDX	Hydrogen-deuterium exchange (mass spectrometry)
HSQC	Heteronuclear single quantum coherence spectroscopy
IMM	Inner membrane of mitochondria
IMS	Inter membrane space (of mitochondria)
KTP	Kinetin triphosphate
LC3	Light chain 3 (microtubule assosciated protein)
LRRK2	Leucine-rich repeat kinase 2
MALDI-TOF	Matrix-assisted laser desorption/ionization-Time of flight (mass spectrometry)
MALS	Multiple-angle light scattering
Mcl-1	Induced Myeloid leukemia cell differentiation protein 1
MDV	Mitochondria-derived vesicles
MOA-A	Monoamine oxidase A
MPP	Mitochondrial-processing peptidase
MTS	Mitochondrial targeting sequence (of PINK1)
NDP52	Nuclear domain 10 protein 52

Nduf10	NADH:ubiquinone oxidoreductase subunit 10
NT	N-terminal linker region (in PINK1)
OMM	Outer membrane of mitochondria
OPTN	Optineurin
PARL	Prenisilins-assosciated rhomboid-like (protein)
PD	Parkinson's disease
PINK1	PTEN-Induced Kinase 1
pUb	phosphorylated ubiquitin (at serine 65 position)
pUbl	phosphorylated ubiquitin-like domain (at serine 65 position)
R0RBR	Parkin construct lacking the N-terminal Ubl domain and linker
RBR	Ring-between ring-ring
RING	Really interesting new gene
SAXS	Small-angle X-ray scattering
SEC	Size-exclusion chromatography
Tc	Tribolium Castaneum
TIM	Translocase of inner membrane (of mitochondria)
TM	Transmembrane
TOM	Translocase of outer membrane (of mitochondria)
TRAP1	Tumor necrosis factor type 1 assosciated protein
TROSY	Transverse relaxation-optimized spectroscopy
Ub	Ubiquitin
Ubl	Ubiquitin-like domain (of Parkin)

UBR	Ubiquitin protein ligase E3 component N-recognin
VDAC	Voltage-dependent anion-selective channel (protein)

Table of Figures

Chapter 1. Introduction

1.1 Parkinson's disease: Features, Causes and Treatments

Parkinson's disease is a debilitating neurodegenerative disorder characterized clinically as a progressive movement disorder whereby patients exhibit motor symptoms including resting tremors, stiffness and gait anomalies. Non-motor symptoms, which are fairly common in Parkinson's patients, though not always present, include autonomic dysfunction (gastrointestinal, urinary and erectile dysfunction) and mental health problems in later stages (dementia and psychotic symptoms) (Grimes et al., 2012). Pathological hallmarks of the disease include a loss of dopaminergic (DA) neurons (involved in motor learning) from the *substantia nigra pars compacta* (SNpc) region of the brain and in most cases the presence of protein deposits in surviving neurons in the vicinity called Lewy bodies that contain aggregated forms of the protein α-synuclein (Dexter and Jenner, 2013). These pathologies are primarily responsible for the observed motor symptoms.

Post-mortem studies have allowed to map the spread of the Lewy pathology across the brain with progression of the disease and allowed an association with the symptoms observed (Braak et al., 2002). Recent work has focused extensively on the cellular and physiological factors that contribute to the occurrence of the disease; work from James Surmeier's group among others, allowed to understand the basis of the selective vulnerability (in terms of morphological and metabolic features) and early loss of SNpc DA neurons to stress and death (and hence the development of Parkinson's pathology) (Surmeier et al., 2010, Surmeier et al., 2011, Pacelli et al., 2015).

Despite these studies, Parkinson's disease is mostly considered a sporadic disease and not much is known about its exact cause. Age and gender are very important factors; epidemiological evidence indicates that 3% of the world population above the age of 65 suffers Parkinson's disease, making it the most common neurodegenerative disease after Alzheimer's

disease (Barreto et al., 2014) with a three times greater prevalence in males than females (Dexter and Jenner, 2013). Environmental risk factors include exposure to mitochondrial toxins and pesticides.

Genetic factors have also been studied, and these include genes that are either directly causative of Parkinson's disease or act as risk factors. The causative genes can be classified into those that cause autosomal recessive or autosomal dominant forms of Parkinson's. Usually the autosomal recessive forms lead to early-onset Parkinson's, while the autosomal dominant forms cause late-onset Parkinson's and hence present more common characteristics to sporadic forms. Also unlike sporadic or late-onset forms, Lewy pathologies are rare in autosomal recessive forms. Examples of genes causing autosomal dominant forms include *PARK1* (α-synuclein) and *PARK8* (LRRK2), while autosomal recessive forms result from mutations in *PARK2* (Parkin), *PARK6* (PINK1) and *PARK7* (DJ-1). In the autosomal dominant forms related to LRRK2, a protein with kinase and GTPase domains/activities, the mutations are associated with increased kinase activity. For α-synuclein, point mutations have been found which promote oligomerization, while gene duplication and triplication events result in increased gene dosage and increase progression and severity of the disease. Autosomal recessive mutations yield loss-of-function of Parkin, PINK1 and DJ-1 proteins (Martin et al., 2011). A multitude of studies show that these three proteins have important neuroprotective roles. Particularly, PINK1 and Parkin work in concert in a common mitochondrial quality control pathway and perform an important neuroprotective function (Trempe and Fon, 2013).

Commonly used treatments for Parkinson's include the use of L-Dopa (a precursor of dopamine; catering for the loss of dopaminergic neurons), MAO-A inhibitors (preventing the oxidation and breakdown of dopamine) and dopamine receptor agonists. The effects of L-Dopa treatment can wear off with time and administration of higher doses can also result in motor complications (dyskinesia and fluctuations). Hence lower doses of L-Dopa are prescribed in combination with other drugs that slow down metabolic degradation, such as (mentioned). Surgical procedures (making ablative lesions) or deep brain electrical stimulation are considered when drug intake fails to alleviate the motor symptoms or complications (Grimes et al., 2012). Nonetheless there is a lack of treatments directly involved in preventing the death of dopaminergic neurons.

1.2 Mitochondrial dysfunction in Parkinson's disease

The association between mitochondria and Parkinson's disease has been known for nearly 30 years now. It owes itself to the appearance of bizarre cases of acute Parkinsonism that were documented in 1982. The victims of this condition were found to be drug addicts who had taken synthesized drugs contaminated with MPTP (1-methyl-4-phenyl-1, 2, 3, 6 - tetrahydropyridine). These patients showed remarkable improvement upon administration of L-Dopa, and in one of the cases, autopsy showed a selective loss of pigmented neurons in the SNpc (Langston and Palfreman, 1995a, Langston and Palfreman, 1995c, Langston and Palfreman, 1995b). It has been found that MPTP is converted by Monoamine Oxidase-B enzyme (MAO-B) to MPP+ (1-methyl, 4-phenylpyridinium), a compound which is a potent inhibitor of the complex I of the electron transport chain in the mitochondria. This can have fatal consequences for the cell either by preventing the development of proton gradients across the mitochondrial inner membrane to produce ATP, or through a disturbance of the of Ca^{2+} ion homeostasis causing activation of Ca^{2+}-dependent enzymes that can induce cellular damage. Complex I is also the target of inhibition by pesticides and chemicals such as rotenone (Sian J, 1999). Mitochondrial DNA (mtDNA) mutations have also been found in the SNpc neurons of patients with Parkinson's disease (Lin et al., 2012). Mitochondrial defects and mtDNA mutations have also been discovered to be associated with the loss of neurons from the SNpc (Reeve et al., 2013). Similarly loss of biochemical activity of complex I in brain tissue from PD patients has also been documented (Schapira et al., 1990). Fairly recently, studies have been conducted which show a direct association between α-synuclein and mitochondria promoting mitochondrial dysfunction (Bir et al., 2014).

1.3 Parkin, PINK1 and Mitochondrial Quality Control

1.3.1 Parkin

Parkin is linked to nearly 50% of all early-onset autosomal recessive cases of Parkinson's. It was one of the first identified genetic factors causing Parkinson's disease; in 1998, a locus linked to autosomal recessive Parkinson's on human chromosome 6 was identified which encoded for a protein having an N-terminus with homology to ubiquitin and a C-terminus with

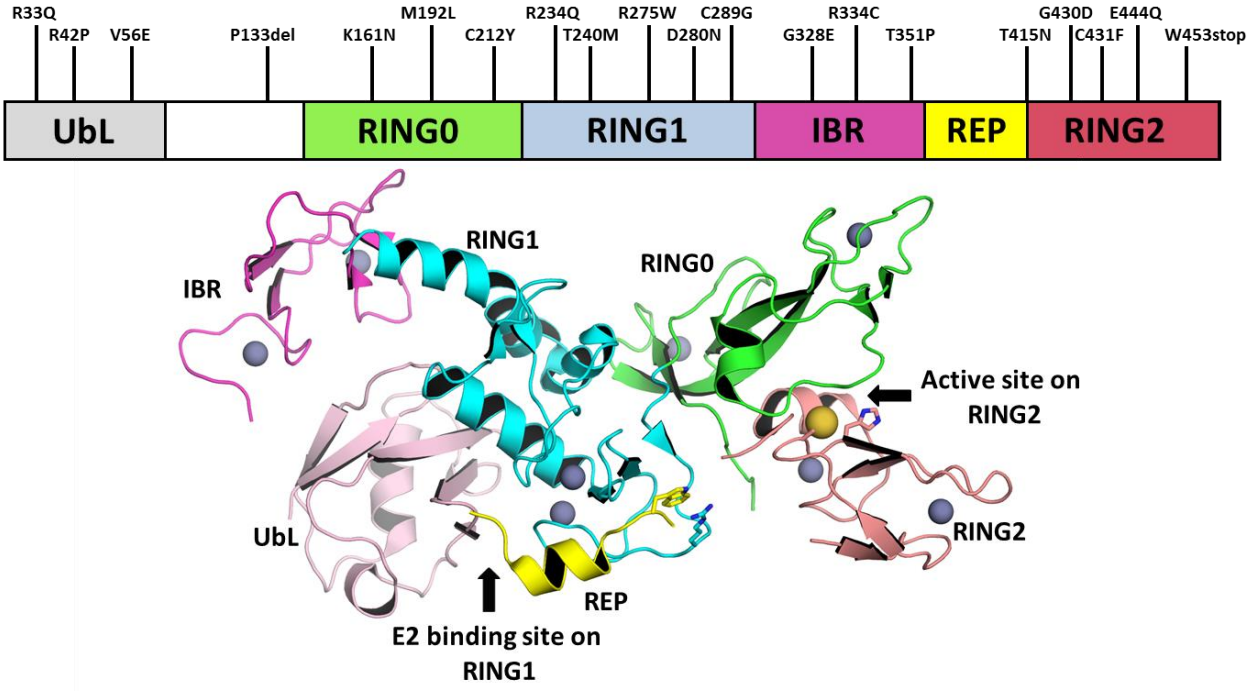

Figure 1.1 **Structure of Parkin** (above) Schematic of the domains of Parkin and some PD-linked mutations that occur in them (below) Structure of full-length parkin adapted from Trempe et al, .2013.

RING-finger motif (Kitada et al., 1998). Later its function as an E3-ubiquitin ligase was established. E3 ligases are enzymes that are involved in the transfer of ubiquitin to a target protein. This process starts with an E1 enzyme (ubiquitin-activating enzyme) which in an ATP-dependent manner first adenylates ubiquitin on its C-terminus and then charges it onto a cysteine on itself with a thioester bond. The ubiquitin in then transferred to a cysteine on an E2 enzyme (ubiquitin-conjugating enzyme). RING-type E3s bind substrates and E2-ubiqutin conjugates (via RING domain) and facilitate the direct transfer of ubiquitin from E2 to substrate. HECT-type E3s (do not have RING domains) accept ubiquitin from the E2 first on an active site cysteine and then transfer the ubiquitin to a substrate. Subsequent studies contributed towards the identification and structural or biochemical characterization of individual domains of Parkin (Tomoo et al., 2008, Beasley et al., 2007, Hristova et al., 2009), and the important discovery that Parkin belongs to the a distinct class of ligases (RBR ligases) that employ a mechanism of ubiquitin transfer which is a hybrid of the RING-type and HECT-type ligase mechanism (Wenzel et al., 2011). In summary, these studies revealed that Parkin is a 52 kDa protein composed of an N-terminal ubiquitin-like (Ubl) domain, linked via a 65 amino acid “linker” region, to the RBR component which includes zinc binding domains RING0, RING1, IBR and RING2 respectively

(Figure 1). Multiple three-dimensional structures of Parkin have been reported since 2013, including full length and truncations lacking the Ubl and/or linker (Trempe et al., 2013, Wauer and Komander, 2013, Riley et al., 2013, Sauve et al., 2015, Kumar et al., 2015). These structures revealed an auto-Inhibited structural form.

This was inferred for two major reasons: the full length structure revealed that the Ubl domain and a small helical linker called the Repressor element of Parkin (REP) (Trempe et al., 2013) occlude the E2 binding interface on RING1, and that the catalytic site on RING2 is occluded by RING0 (Figure 1). These findings implied the need for multiple conformational changes to occur in order to enable ubiquitin transfer from the E2 to Cys431 on RING2. Unlike most E3 ligases, Parkin can build a variety of ubiquitin chain types including M1, K6, K11, K27, K29, K48 and K63 on its substrates and it can also target a variety of substrates (Durcan et al., 2011, Ordureau et al., 2014). It is worth mentioning that PD-related mutations are present in all domains of Parkin (Figure 1). Hence all the domains play an important structural or functional role in the protein. Studies have also shown that in the neurons of PD patients or neurons treated with oxidants or stress agents, Parkin also found more in the insoluble cellular fractions compared to normal cells (Wang et al., 2005). Parkin has also been reported as a phosphorylation target for PINK1 on its UbL domain at Ser65 for its activation (Kondapalli et al., 2012). c-Abl has also been reported to phosphorylate Parkin on RING0 at Tyr143 (Imam et al., 2011) for its inhibition though the finding remains controversial. In terms of cellular function, Parkin has been shown to play key roles in protective response to apoptotic stress, intracellular pathogens (Manzanillo et al., 2013), mitochondrial quality control and motility (Trempe and Fon, 2013, Wang et al., 2011), EGFR trafficking and internalization (Fallon et al., 2006) and endocytic vesicular trafficking (Trempe et al., 2009). The diversity of Parkin's substrates and cellular functions suggests that Parkin acts as a key E3 ligase in the cell signaling network.

1.3.2 PINK1

PINK1 was originally described as a gene whose expression was compromised in ovarian cancer (Unoki and Nakamura, 2001) and later was found to be a mitochondrially-located kinase that protects cells from apoptotic stress and is linked with autosomal recessive Parkinson's disease (Valente et al., 2001, Valente et al., 2004). Human PINK1 is a 581 amino acid serine\threonine

protein kinase with an N-terminal mitochondrial targeting sequence, followed by a transmembrane segment (TM), an N-terminal linker region (NT), a canonical bi-lobular kinase domain and a C-terminal region (Trempe and Fon, 2013) (figure 2). PD-linked mutations are found in all domains of the PINK1 protein (Cardona et al., 2011).The mitochondrial targeting sequence has been inferred based on homology and found to be positively charged in nature, which would facilitate the import across the mitochondrial inner membrane. It has been proposed that PINK1 might have two mitochondrial localization signal peptides, in the regions 1-34 and 70-94, both of which are on their own capable of localizing PINK1 to mitochondria (Zhou et al., 2008, Okatsu et al., 2015). PINK1 import into mitochondria involves its interactions with the TOM (Translocase of the Outer Membrane of mitochondria) and TIM (Translocase of the Inner Membrane of mitochondria) complexes on the outer membrane and inner membrane of the mitochondria respectively. Accumulation of PINK1 and its activation on the outer mitochondrial membrane requires complex formation with TOM (Lazarou et al., 2012); TOM40 (the channel subunit of TOM) (Okatsu et al., 2015) and TOM7 (Hasson et al., 2013) have been shown to be important for import and stabilization of PINK1 on the OMM respectively. A report has indicated the PINK1 might exist as a dimer in complex with TOM (Okatsu et al., 2013). As PINK1 N-terminus gets imported through the TIM complex, it is cleaved at an unknown site by MPP in the mitochondrial matrix (Greene et al., 2012). The TM of PINK1 has been predicted to be an α-helical segment more than 20 amino acids in length, which is a target of cleavage by the rhomboid protease PARL between Ala103 and Phe104 (Deas et al., 2011, Jin et al., 2010). The TM domain is also considered to harbor a ‘stop-transfer’ signal to prevent further translocation of the protein into the matrix and can allow for PINK1 to stay anchored to the IMM or released into the IMS (Okatsu et al., 2015, Sim et al., 2012).

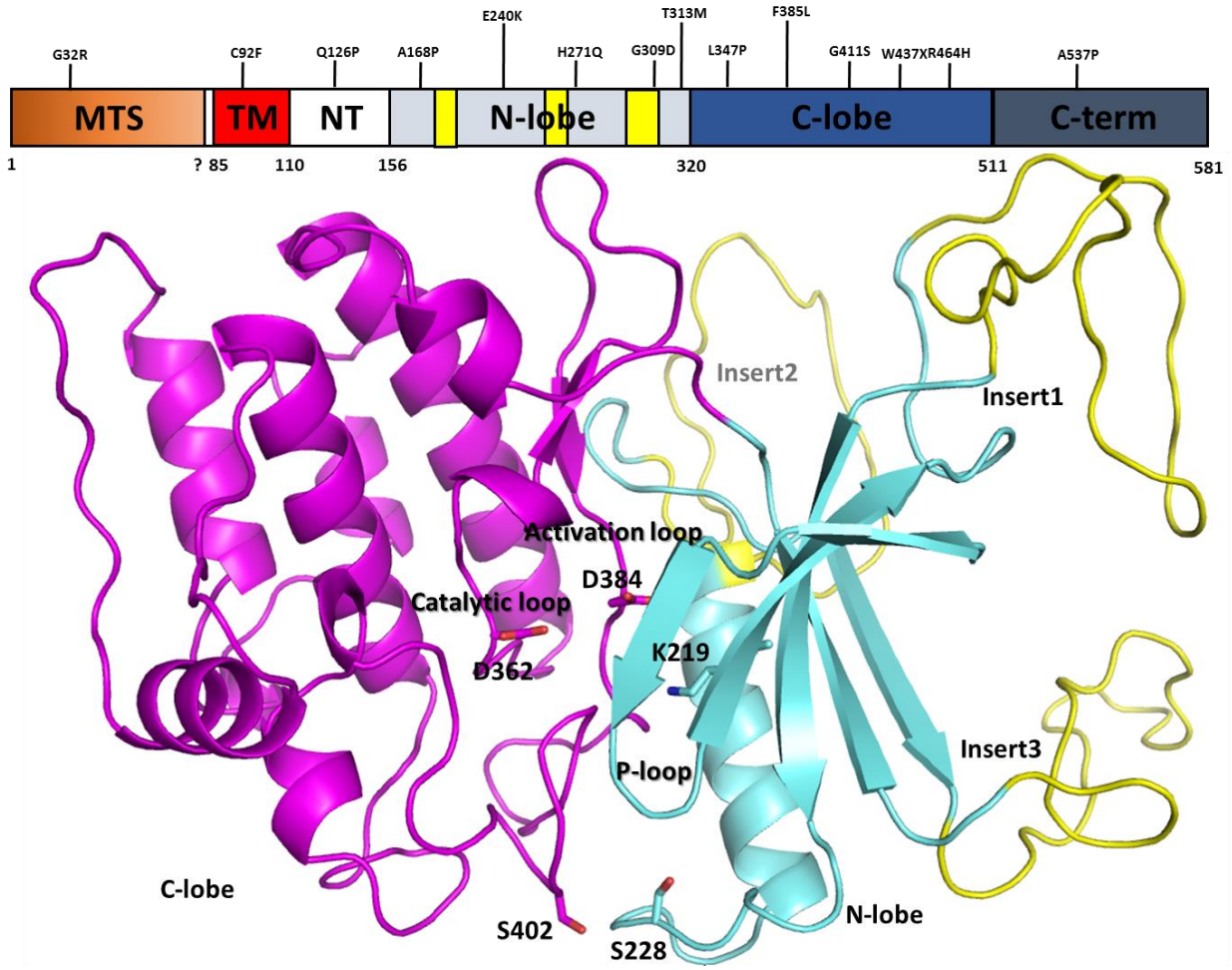

Figure 2.2 **Domain Organization of PINK1** (Above) Domains of PINK1 and some PD-linked mutations (Below) homology model of human PINK1 kinase domain (residues 156-511) [40] showing the insert regions, conserved catalytic motifs and residues (K219, D362 and D364) and proposed autophosphorylation sites (S228 and S402) [52].

The final 52 kDa form of PINK1 has also been found to be targeted by UBR1, UBR2 and UBR4 E3 ligases for proteasomal degradation via the N-end rule pathway in the cytoplasm (Yamano and Youle, 2013). It has been suggested that cytoplasmic PINK1 might also have a cytoprotective role (Lim et al., 2015). Multiple PD-linked mutations are found in the MTS and TM region and are thought to disrupt the structural and sequence features required for mitochondrial targeting or processing by the mentioned enzymes (Cardona et al., 2011, Sim et al., 2012).

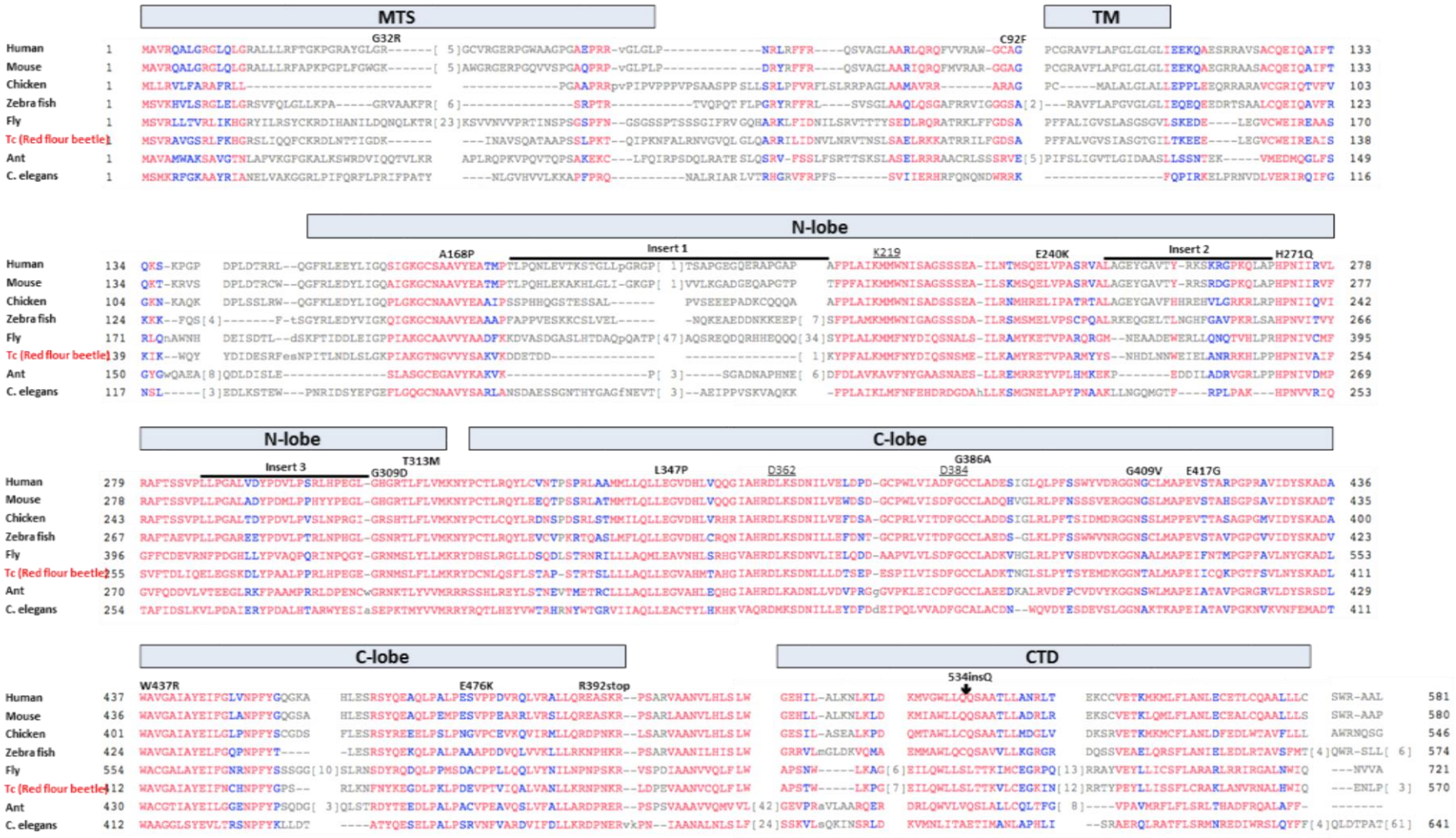

Figure 1.3 **Multiple sequence alignment of PINK1 orthologs**. Blue bars indicate segments in PINK1 Inserts in the kinase domain have labelled with black line. Active site residues and some PD-linked mutations in labelled. The insertion site for the PD-mutation 534insQ is indicated with a black arrow.

The kinase domain of PINK1 was found to be homologous to the Calcium/Calmodulin-dependent kinase (CamK) family of kinase. The reported homology model and sequence homology studies with the CamK family show a conservation of structural and sequence features key to catalysis including the P loop (162-165 involved in phosphate binding), Lys129 in the AIK motif (involved in ATP orientation), Asp362 in the HRD motif (catalytic aspartate in the catalytic loop) and the conserved DFG motif (part of the activation loop involved in magnesium ion coordination) (Figure 1.2 and 1.3) (Cardona et al., 2011). The motifs lie at the interface of the N and C lobes of the kinase domain and form a cleft for ATP binding. Autophosphorylation sites (S228, T257and S402) have been reported for PINK1 (Kondapalli et al., 2012, Okatsu et al., 2012), though the role of autophosphorylation for the activation of PINK1 remains controversial. For example, the reported S402A mutant (located in the activation loop) which supposedly impaired PINK1 activation (Okatsu et al., 2012), was later found to render the enzyme temperature-sensitive as opposed to deactivated due to lack of autophosphorylation (Narendra et al., 2013). PD-linked mutations in the kinase domain of PINK1 are thought to reduce the enzymatic activity or compromise its structural integrity (Cardona et al., 2011).

PINK1 also harbors unique features as a kinase including the NT, the insertions (1-3) in the N-lobe of the kinase domain and the C-terminal region (Trempe and Fon, 2013). All these regions harbor PD-linked mutations (Cardona et al., 2011). Since these regions do not share homology with any other known proteins, structural and functional features have not been inferred. Compared to the kinase domain, these regions are also less conserved across orthologs of PINK1; PINK1 from the insect species *Tribolium castaneum* (red flour beetle) and *Pediculus humanus corporis* (louse) possess a much shorter insert1 (figure 1.3), while for *Drosophila melanogaster* (fruit fly) insert1 is much longer than human PINK1 (Woodroof et al., 2011). A report shows that PINK1 recognizes and hydrolyzes KTP (kinetin triphosphate) more preferably than ATP, and it has been hypothesized that these inserts in the kinase domain are responsible for specificity (Hertz et al., 2013). Insect orthologs of PINK1 have also been found to be more active kinases than human PINK1 (Woodroof et al., 2011). The C-terminal region has been shown to have a regulatory role for the kinase domain, though whether it inhibits or activates the kinase domain is unclear (Sim et al., 2006, Silvestri et al., 2005). Secondary structure

predictions indicate that the C-term region is composed of a-helices and disordered loops (Sim et al., 2012).

PINK1 has been reported by different groups to phosphorylate different substrates including the mitochondrial chaperone TRAP1 (Pridgeon et al., 2007), Miro (Wang et al., 2011), Mitofusin2 (Chen and Dorn, 2013), Nduf10 (complex1) (Morais et al., 2014) and also causes indirect phosphorylation of Rab8A (Lai et al., 2015). A peptide library screening study identified that PINK1 prefers to phosphorylate substrates with a proline residue downstream of the phosphorylation site (p+1) (Woodroof et al., 2011). However, despite these studies, the best-documented substrates of PINK1 are Parkin on its Ubl domain (Kondapalli et al., 2012, Shiba-Fukushima et al., 2012) and ubiquitin (Koyano et al., 2014, Kazlauskaite et al., 2014, Kane et al., 2014), that are involved in the mitochondrial quality control pathway.

1.3.3 PINK1/Parkin Mitophagy pathway

Neurons rely critically on mitochondria for efficient functioning due to high energy demands and because mitochondria are responsible for buffering the high calcium influx (e.g. due to nerve impulse transmission). These processes can make mitochondria vulnerable to damage, and so for neuron survival and functioning, mitochondrial quality control and maintenance is very important. The PINK1/Parkin pathway is one of the best known pathways involved in mitochondrial repair and removal of damaged mitochondria (Grenier et al., 2013).

The first phenotypic studies relating PINK and Parkin to Parkinson's disease came from drosophila; PINK1 mutants produced motor dysfunction phenotypes in drosophila including defects in climbing and flying ability, wing and flight muscle defects and some decrease in the number of dopaminergic neurons (Park et al., 2006), and electron microscopy studies indicated that PINK1 and Parkin null flies exhibited defects in mitochondrial morphology (Clark et al., 2006). Furthermore it was shown that the defects in PINK1 null flies could be rescued by Parkin overexpression and not vice versa, showing that Parkin acted downstream of PINK1 in this mitochondrial maintenance pathway. In mammalian cells, Parkin was later found to be recruited to mitochondria when they are damaged by dissipating the membrane potential using CCCP, a proton ionophore (Narendra et al., 2008). Parkin recruitment to mitochondria is PINK1 kinase activity-dependent (Narendra et al., 2010); depolarization inhibits PINK1 translocation

across the mitochondrial membranes and its proteolytic processing by MPP and PARL, resulting in its accumulation on the OMM in complex with TOM where it can recruit Parkin. Subsequently Parkin was identified as a phosphorylation target of PINK1 (at Ser65 on the UbL domain) (Kondapalli et al., 2012). However since S65A mutant of Parkin was not fully impaired in terms of mitochondrial recruitment (Shiba-Fukushima et al., 2012), but PINK1 kinase-dead mutants are fully impaired, there had to exist another PINK1 kinase-dependent substrate that could enable Parkin recruitment. This substrate was found to be ubiquitin; PINK1 phosphorylates Ub directly following depolarization of mitochondria, which is responsible for Parkin's recruitment to mitochondria and its phosphorylation by PINK1. *In vitro,* phosphorylated ubiquitin *(*pUb) was shown to increase Parkin's activity (Koyano et al., 2014, Kane et al., 2014, Kazlauskaite et al., 2014). Activated Parkin recruits to mitochondria and polyubiquitinates OMM proteins including Mitofusin2 and VDAC (Geisler et al., 2010, Sarraf et al., 2013). These chains can get phosphorylated further and recruit more Parkin, which would then get phosphorylated by PINK1 and get activated, hence forming a positive feedback loop and a feedforward amplification of the signal (Ordureau et al., 2014, Ordureau et al., 2015). Whether Parkin phosphorylation or Ub phosphorylation is the first step in the pathway is still unclear. Buildup of polyubiquitin chains on substrates is followed by the recruitment of cargo receptor proteins including NDP52, OPTN and p62 to mitochondria (Lazarou et al., 2015, Heo et al., 2015) ; these proteins bridge ubiquitinated proteins (on the mitochondria) to the ubiquitin-like proteins LC3B and LC3C, eventually resulting in the recruitment of autophagy machinery to mitochondria to initiate mitophagy (Lazarou et al., 2015, Rogov et al., 2014). The process has been illustrated in Figure 1.4. Hence PINK1 and Parkin are the necessary initial steps required for response to mitochondrial damage, though one group has shown recently that mitophagy can occur in the absence of Parkin, but not PINK1 (Lazarou et al., 2015).

It has been shown that the mitochondrial morphology defects that occur due to defects in PINK1 and Parkin can be rescued by an increase in the mitochondrial fission-promoting protein Drp1 and a decrease in the fusion-promoting protein Mitofusin (Poole et al., 2008). Since the activation of the PINK1/Parkin pathway targets the removal of Mitofusin (Poole et al., 2010), it shifts the balance towards mitochondrial fission to isolate and removes damaged parts of the

mitochondrial network. PINK1 and Parkin have also been shown to target Miro (a protein that links mitochondria to kinesin and dynein motors for transport along microtubules) for removal, possibly to prevent the transport of damaged mitochondria and for efficient quarantine and removal (Wang et al., 2011).

The PINK1/Parkin mitophagy pathway has been recapitulated by the use of other mitochondrial damaging insults including the use of rotenone (complex I inhibitor: prevents electron transfer to ubiquinone), Antimycin A (complex III inhibitor: prevents electron transfer to cytochrome C protein) and (ATP synthase inhibitor; prevents reverse ATP synthase from building up H^+ gradient) oligomycin (Lazarou et al., 2015), valinomycin (K^+ uncoupler) (Zhang et al., 2014) and accumulation of unfolded proteins in the matrix (Jin and Youle, 2013) (among others). PINK1 is thus a sensor to a wide variety of mitochondrial damages.

The PINK1/Parkin pathway has also been shown to sense the amount of damage to produce different kinds of cellular outcomes. While mitochondrial depolarization can trigger mitophagy, it was shown that under mild oxidative stress, PINK1 and Parkin induce the production of MDVs which carry damaged cargo directly to the lysosome instead of initiating mitophagy on whole mitochondria (McLelland et al., 2014). On the other hand, a report suggests that higher levels of damage can cause PINK1 and Parkin to initiate apoptosis by removal of the anti-apoptotic protein Mcl-1 (Zhang et al., 2014).

1.4 Objectives

PINK1 is a mitochondrial damage sensing protein whose ubiquitin and Ubl kinase activity is required for Parkin activation and neuroprotection. How PINK1 selectively recognizes and phosphorylates these substrates in not understood. As the first member of the ubiquitin kinase family, we have no structural model for how a kinase can selectively engage ubiquitin. Moreover, why PINK1 specifically recognizes the Parkin Ubl and Ub and not other ubiquitin-like domains isn't understood (Kazlauskaite et al., 2014). In this study, I sought to characterize the PINK1 protein structurally and functionally. Despite the fact that PINK1 has been rigorously studied in cell-based assays and in some cases *in vitro* biochemical assays, there was a lack of a recombinant expression systems for PINK1 for *in vitro* structural and functional studies. Only a

few studies have considered orthologs of PINK1 for substituting human PINK1 in *in vitro* functional [54]. Similarly, there is not much information available on the expression of individual domains of PINK1. In this study I have tried to explore orthologs of PINK1 in terms of their expression to provide a suitable target to perform structural studies. On the structural side, besides the lack of an experimental structure of PINK1, there is no information available on the oligomeric state of PINK1 in solution and component of the protein that can potentially regulate oligomerization. We have investigated this using size-exclusion chromatography (SEC) and multiple-angle light scattering (MALS).

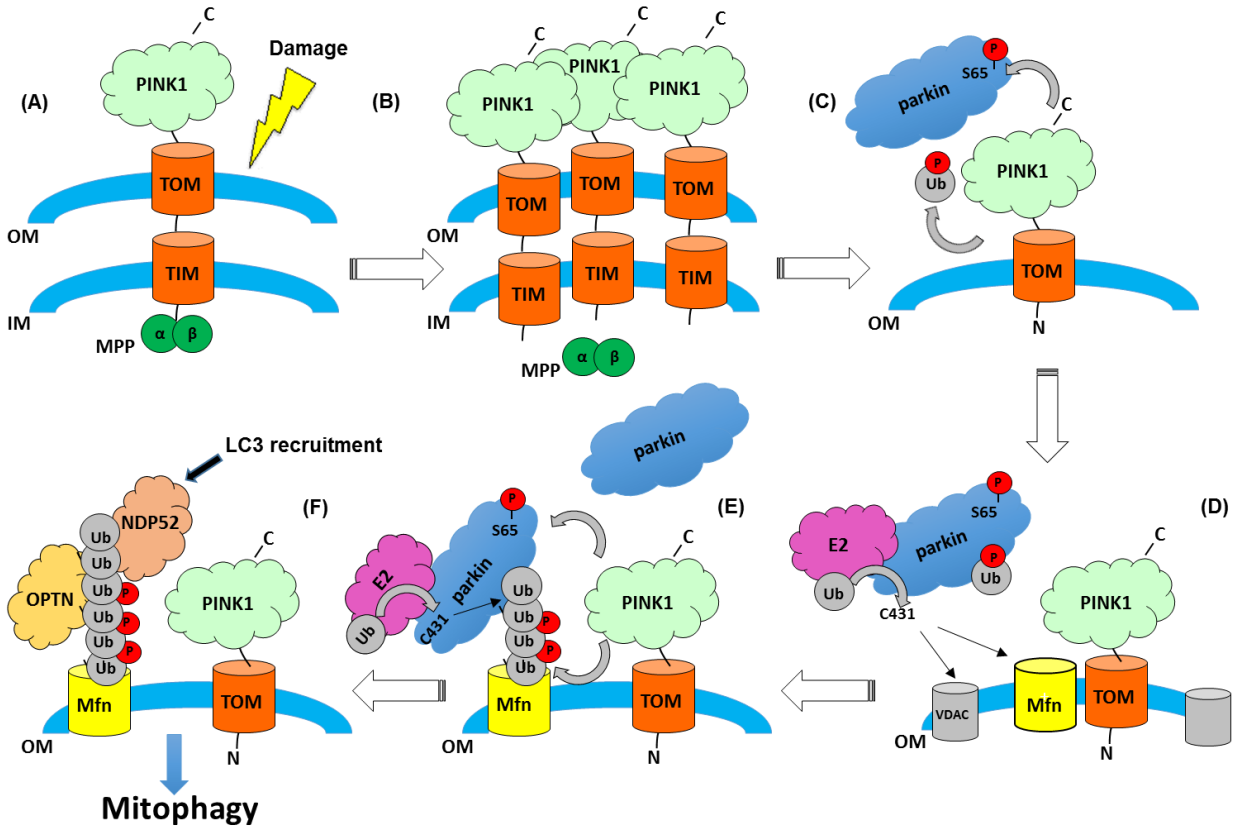

Figure 1.4 **The PINK1/Parkin Mitophagy Pathway** (A) Mitochondrial damage due to depolarization causes (B) PINK1 accumulation on mitochondria in complex with TOM. (C) PINK1 phosphorylates Parkin and Ub (D) both of which result in Parkin's E3 ligase activation and consequent ubiquitination of substrates on mitochondria like Mitofusin (Mfn). (E) Ubiquitin chains built by Parkin get phosphorylated by PINK1 to recruit more Parkin and initiate a feed-forward cascade. (F) Build-up of ubiquitin chains also recruits autophagy receptors OPTN and NDP52 and eventually the recruitment of mitophagy machinery.

On the functional side, while PINK1 has extensively studied in cells to study Parkin recruitment, there is a lack of *in vitro* functional studies to study Ub and Parkin UbL phosphorylation. In particular, the effect of PD-linked mutations on Ub has not been explored. The enzymatic activity of PINK1 has not previously been characterized in terms of kinetics towards its substrates (Ub and Ubl), and hence its preference for one substrate over the other has not been elucidated. In this study I have deployed a Phos-tag SDS PAGE technique to study PINK1 substrates phosphorylation and investigate the differences in enzyme kinetics. Since PINK1 specifically targets Parkin Ubl and Ub for phosphorylation both which contribute an important physiological phenomenon, it is important to understand which sequence and structural features of these substrates are important for recognition by PINK1. I have employed the use of 2D NMR techniques and phosphorylation assays to get to understand this.

In terms of Parkin phosphorylation by PINK1, while it has been shown that Ub phosphorylated by PINK1 has an important role to play in the activation of Parkin, the precise molecular nature of this activation i.e. conformational change in Parkin needed for activation needs to be understood. We have tackled this question using *in vitro* phosphorylation assays, SAXS and NMR studies and used it to elucidate the precise role of pUb and phosphorylation of Parkin in its activation.

This thesis is a highlight of my investigation on PINK1 over the course of my Master's residency. Chapter 2 of the thesis is a summary of the methods employed for investigation. Chapter 3 deals with my work on the expression of PINK1 and its orthologs as well as a brief investigation on the dimerization on PINK1. Chapter 4 deals with PINK1 phosphorylation and binding to Ub and Ubl, with a brief investigation of PINK1's nucleotide binding affinities. Chapter 5, which is a part of a published work from my lab (Sauve et al., 2015), is an investigation of Parkin's activation by PINK1 and pUb. Finally, chapter 6 highlights conclusions that can be drawn from this thesis work and discusses about potential future investigations.

Chapter 2. Materials and Methods

2.1 Recombinant protein expression and purification

2.1.1 PINK1 cloning, expression and purification:

All PINK1 constructs were expressed as N-terminal GST-tagged proteins from pGEX-6p-1 vector. Human PINK1 constructs (111-581 and 148-581) were provided by Veronique Sauvé (Gehring lab). cDNA for full-length TcPINK1 (codon-optimized for E.coli expression) was ordered from Invitrogen. Primers were designed to clone TcPINK1 (full length, 121-570 and 128-570) or the C-terminal regions of human PINK1 (514-581) and TcPINK1 (487-570), using the BamHI and XhoI restriction sites in the vector. The cloning (restriction, ligation and transformation) was carried out according to standard protocol. Point mutations (E127K, G285D, D359N, C362S, C363S and K513P) and deletions in TcPINK1 (to generate 143-570 construct) or human PINK1 (Δ181-209 or Δ184-206) were made using the Quikchange site-directed mutagenesis method (Agilent). Gibson assembly method (NEB) was used to generate TcPINK1 constructs to generate deletions of C-terminal regions (143-486 and 143-500). All cloned vectors were expressed in BL21 DE3 cell lines (NEB) in Terrific Broth at 37 °C up to an O.D of 1.0, after which they were incubated at 16 °C, induced with 100 μM IPTG and left to express protein at 16 °C overnight. Cells were harvested and lysed via sonication in lysis buffer (50 mM Tris, 300 mM NaCl, 3 mM DTT, 0.1 mg/ml lysozyme, 25 μg/ml DNase I, 5 mM $MgSO_4$, protease inhibitors (Roche) and 0.5% Tween at pH 8.0). The lysate was clarified by centrifuging at 18,000 rpm for 45 min in a Sorvall SS-34 rotor. Glutathione-sepharose resin was used to bind GST-tagged protein in binding buffer (50 mM Tris, 300mM NaCl, 3 mM DTT pH 8.0) for 60 min on a rotating platform at 4 °C. After washing with the binding buffer, the protein was eluted with elution buffer (50 mM Tris, 300 mM NaCl, 20 mM Glutathione, 0.1% CHAPS and 3 mM DTT pH, 8.0) and concentrated using Amicon-Ultra concentrators (10000 M.W. cut-off; EMD Millipore). To remove the GST tag, 3C protease (1:50 protease-to-substrate ratio) was incubated with the protein overnight at 4 °C; control samples were also stored at 4°C and -80°C without cleavage for comparison. The protein was first purified using the anion-exchange column MonoQ (GE healthcare) to get rid of excess GST, and then further purified by size-exclusion chromatography using Sephacryl S200 or

Superdex S200 (GE healthcare) connected in series with a GST trap 4B (GE healthcare) to remove the GST. The obtained pure protein was concentrated as described above. Protein concentrations were measured using the Bradford assay, standardized with bovine serum albumin solutions. Protein expression was analyzed using SDS-page gels.

2.1.2 Parkin, Ub and Ubl expression

Constructs containing His_6-tagged ubiquitin (wild type or S65A) were provided by Noriyuki Matsuda (Tokyo Metropolitan Institute of Medical Science, Tokyo). These constructs were expressed in BL21 DE3 cells grown in Terrific Broth at 37 °C uptil an O.D of 0.9 after which they were incubated 16^{o}C, induced with 500 μM IPTG and left to express protein at the latter temperature overnight. Harvesting and lysis steps were performed as described in the previous section with lysis buffer (50 mM Tris, 100 mM NaCl, 0.1mg/ml lysozyme, 25 μg/ml DNase I, 5 mM $MgSO_4$, protease inhibitors and 0.5% Tween at pH 7.5). Ni-NTA (QIAgen) resin was used to bind His-tagged protein in binding buffer (50 mM Tris, 100 mM NaCl pH 7.5) for 30 min on ice. After washing (with 50 mM Tris, 300 mM NaCl pH 7.5), the protein was eluted (using 50 mM Tris, 100 mM NaCl and 120 mM Imidazole pH 7.5). Pure His-tagged protein was obtained after a size-exclusion chromatography run using Superdex 75 (GE Healthcare) equilibrated in binding buffer and concentrated to the desired concentration using Amicon-Ultra concentrators (3000 M.W. cut-off; EMD Millipore).

Full-length rat Parkin and its point-mutants (L266K and H302A) had previously been cloned into pGEX-6p-1 (as GST-fusion proteins). The expression and purification of these constructs were performed as described in Trempe *et al*. 2013 (Trempe et al., 2013). Ubl domain of Rat Parkin (1-76) and ubiquitin had previously been cloned in pGEX-6p-1. Point mutations in Ubl (R6A, I44A, K48A, Q71A, R72A and H68A) were made using the Quikchange site-directed mutagenesis method (Agilent). Expression and purification (as GST-fusion proteins) of these proteins was performed as described in Trempe *et al*. 2009 (Trempe et al., 2009), except for the growth of bacteria that was done in Terrific Broth. Expression of ^{15}N-labelled Ubl was performed in M9 minimal media supplemented with $^{15}NH_4Cl$ for NMR experiments, as described (Trempe et al., 2009). Protein concentrations were measured using UV absorbance.

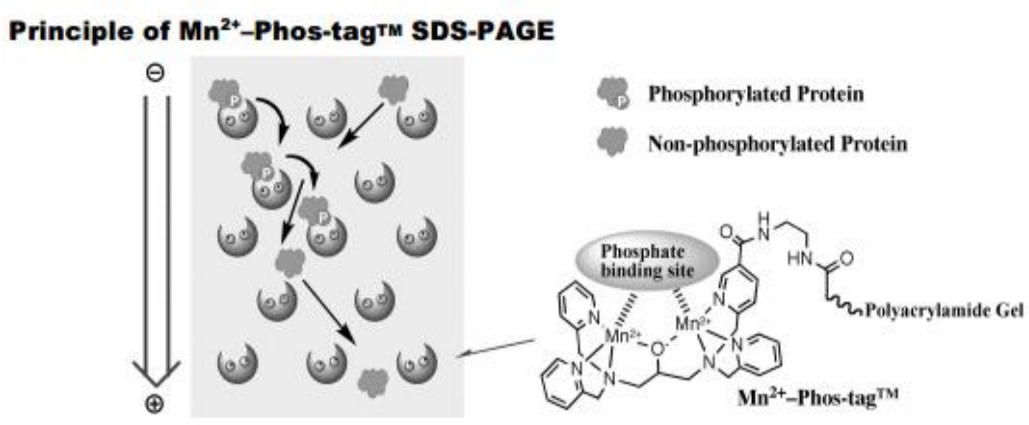

Figure 2.1 Principle of Phos-tag gel system (copied from manufacturer's manual).

All sequences were verified using DNA sequencing by the McGill University and genome Quebec innovation center at McGill University, using standard pGEX forward and reverse primers.

2.1.3 Small scale expression test of other PINK1 orthologs

PINK1 constructs of TcPINK1 (143-570), *Gallus gallus* (137-600), *Camponotus floridanus* (132-162), *Pediculus humanus corporis* (118-575), *Dendroctonus penderosae* (123-570) and *Crassostrea gigas* (118-600), cloned in pGEX-6p-1 constructs were expressed in E. coli DE3 cells and cultured in 15 ml LB. All these constructs correspond to regions of PINK1 following the transmembrane helix. Purifications were performed the same way as described in 2.1.1. Elutions from the purifications were analyzed by loading on SDS-PAGE gel.

2.2 Kinase assays

2.2.1 Detection of Ubiquitin phosphorylation

Kinase reaction was performed with or without 2.5 μM of GST-TcPINK1 (128-570), 50 μM His-Ub (wild type) or His-Ub (S65A), 1 mM ATP and 2 mM $MgSO_4$, in kinase buffer composed of 50 mM Tris, 100 mM NaCl and 1 mM DTT (pH 7.5), for 30 minutes at 30°C. The reactions was quenched with SDS-Page gel loading buffer and 10 μL of the reaction was loaded on 15% Tris- glycine gels with 20 μM Phos-tag™ (Wako, Japan) and 40 μM $MnCl_2.6H_2O$ (in the resolving gel). Phos-tag is a compound that forms complexes with divalent metal ions such as Mn^{2+}, which can coordinate phosphate groups on proteins (manufacturer's description). Addition of the compound cross-linked to the resolving gel results in the selective retardation of

phosphorylated protein compared to non-phosphorylated species (figure 2.1). For mass spectrometry analysis, a similar phosphorylation reaction was performed except with 10 μM His-Ub with or without 10 mM ATP. 20 μL of each reaction was prepared for intact protein MALDI-TOF mass spectrometry using C18 Ziptips using the manufacturer's protocol (Millipore EMD). The final product was eluted in 5 μl of 0.1% formic acid and 80% acetonitrile, of which 1 μl was spotted on the target matrix along with 1 μl of sinapinic acid.

2.2.2 Optimization of the Phos-tag gel system

Optimization was performed on the Phos-tag gel system to allow for quantitative analysis for kinetic analysis of phosphorylation of Ub and Ubl. Since Tris-tricine gels resolve proteins of sizes smaller than 30 kDa better than Tris-glycine gels (Schagger, 2006), they were tested in combination with 20 μM Phostag and 40 μM $MnCl_2.6H_2O$ to analyze Ub phosphorylation. However no mobility shift was detected for His-Ub following ATP-dependent phosphorylation by PINK1 (Figure 2.2A, lane 1 and 2 are the same compared to controls lanes 3, 4 and 5). Since Tris-tricine gels use different concentrations and pH of Tris compared to Tris-glycine gels (among other things), these factors might alter the migration of phosphorylated proteins in the presence of Phos-tag. As mentioned in the previous section, divalent cations such as Mn^{2+} are essential for Phos-tag gels to work since they bind to both Phos-tag and the phosphate groups on proteins simultaneously to retard their migration. I asked if changing the cation to another divalent cation (transition metal) could allow the detection of phospho-protein; Tris-tricine gels were run with the same kinase reactions as Figure 2.2 (A) but this time with Zn^{2+} as the cation instead of Mn^{2+} (Figure 4.2 B). Lane 6 and 7 show the mobility shifts in an ATP and TcPINK1 dependent manner compared to controls (lane 8, 9 and 10). Also, it can be seen that the phosphorylated and non-phosphorylated bands are sharper and well-resolved. To further increase their separation, Phos-tag and Zn^{2+} can be increased to 30 μM and 60 μM respectively, and such conditions were used in kinetics assays shown below (Fig. 4.4 for

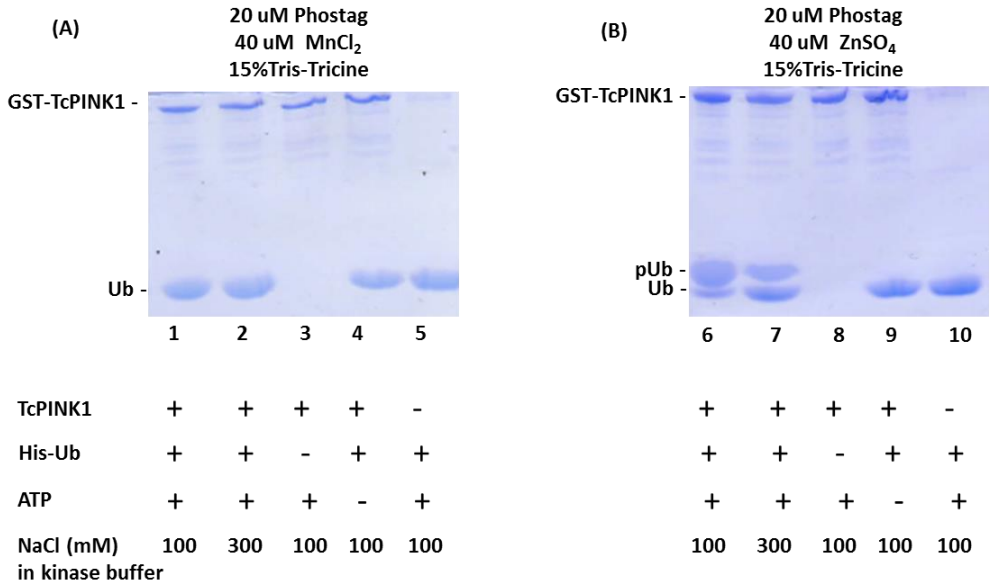

Figure 2.2 **Optimization of Phos-tag Gel System** TcPINK1(143-570) kinase assays with His-Ub using different salt concentrations in kinase buffer and analyzed using Phos-tag Tris-Tricine gels with (A) $MnCl_2.6H_2O$ or (B) $ZnSO_4$.

instance). All the phosphorylation assays of Ub with 15% Tris-Tricine reported in this thesis use these concentrations of Phos-tag and Zn^{2+}. I also investigated the effect of increasing NaCl concentration in the reaction buffer on the kinase activity. A concentration of 100 mM NaCl was found to yield more pUb than 300 mM NaCl in the buffer conditions (compare lane 6 with lane 7). This is an important finding since the salt concentration optimal for purification is 300 mM NaCl, but as shown previously (section 2.1.1) these conditions are not optimal for pUb phosphorylation.

2.2.3 Ubl phosphorylation assays

Phosphorylation assays of GST-UbL and its mutant forms were performed using 2 μM GST-TcPINK1 (143-570) and 30 μM substrate with 1 mM ATP and 2 mM $MgSO_4$ for 5 min. These samples were loaded on 12% Tris-Tricine gels with 30 μM phos-tag and 60 μM $ZnSO_4$, which were stained with Coomassie Brilliant Blue. Phosphorylation of the Ubl (non-fusion form) was performed similarly for 15 min with TcPINK1 (121-570) or TcPINK1 (143-570).

2.2.4 Phosphorylation assays with PD-mutant forms of TcPINK1

Phosphorylation assays with different mutant forms of TcPINK1 were performed with 2.5 μM of the enzyme and 120 μM His-Ub for 30 minutes. The sample were loaded on 15% Tris-

tricine gels with 30 μM Phos-tag and 60 μM $ZnSO_4$, which were stained with Coomassie Brilliant Blue.

2.2.5 Kinetics of Ub and UbL phosphorylation

For Michealis-Menten kinetic analysis, time course experiments were performed with 120 μM His-Ub with 2.5 μM GST-TcPINK1 (143-570) or 120 μM Ubl with 1.25 μM GST-TcPINK1 (143-570) for 2, 5, 10 and 20 min. The samples were loaded on 15% Tris-tricine gels with 30 μM phos-tag and 60 μM $ZnSO_4$and stained with Coomassie Brilliant Blue. Densitometry was done using ImageJ following destaining to quantify band intensities of phosphorylated species. These were plotted (after background subtraction and normalization with respect to substrate concentration) against time to determine the time points that can be used for initial rate (v_o) determinations (in Microsoft excel). Experiments were then done to obtain K_m and V_{max} parameters for Ub phosphorylation by performing phosphorylation reactions for 5 min at different substrate concentration for both His-Ub and Ubl. These experiments were performed at 2.5 μM and 5 μM enzyme for His-Ub. For Ubl phosphorylation, two replicates of the experiment were performed at 2 μM enzyme concentration. Following gel runs and densitometry, the intensities (v_o) were plotted as a function of concentration and the values for K_m, V_{max} and k_{cat} were obtained from the global fit to the two datasets using the data analysis software Prism. For either substrate, the intensities were normalized with respect to the substrate concentration and time (in units of μM/min) and scaled according to the enzyme concentration before performing the analysis. Control samples of His-ubiquitin and Ubl were loaded on gel at different concentrations to demonstrate a linear relationship between concentration and intensity measurement by densitometry. To determine the K_m of phosphorylation with respect to ATP, kinetic experiments were performed as mentioned above with an excess of His-Ub (1 mM) and a range of ATP concentrations.

2.2.6 Parkin phosphorylation assays and Kinetics

Parkin phosphorylation assays were performed with 0.1 μM GST-TcPINK1 (143-570) with 3 μM Parkin WT, L266K or H302A as substrates in the presence or absence of 3 μM pUb and 1 mM ATP in a reaction volume of 25 μL. The kinase buffer constituted 50 mM Tris-HCl, 100 mM NaCl, 1 mM DTT and 2 mM MgSO4. Reactions were performed for 5 min at 30 °C and were

quenched using SDS PAGE loading buffer and 20 μL of the reaction was loaded on 10% Tris-Glycine gels containing 20 μM Phostag and 40 μM $MnCl_2.4H_2O$. Gels were stained with Coomassie Brilliant Blue for visualization.

To compare the effects of pUb or Ub S65A on Parkin phosphorylation, assays were performed with 0.1 μM GST-TcPINK1 (143-570) with 30 μM Parkin WT in the presence or absence of 30 μM pUb or 30 μM UbS65A and 1 mM ATP in a reaction volume of 25 μL. The kinase buffer constituted 50 mM Tris-HCl, 100 mM NaCl, 1 mM DTT and 2 mM MgSO4. Reactions were performed at 30 °C and at each time point (2 min or 10 min), 8 μL was taken and quenched using 4 μL SDS PAGE loading buffer. After denaturation, 2 μL of the latter mixture was loaded on 10% Tris-glycine gels containing 20 μM Phostag and 40 μM $MnCl_2.4H_2O$. Gels were stained with Coomassie Brilliant Blue for visualization.

For kinetics of Parkin phosphorylation (wild type or L266K), experiments were performed as mentioned in section 2.2.5 with 2 μM GST-TcPINK1 (143-570).

2.3 ITC experiments

2.3.1 ITC experiment for TcPINK1 and AMP-PNP binding

The ITC buffer consisted of 50 mM HEPES, 300 mM NaCl, 0.5 mM TCEP and 5 mM $MgSO_4$ at pH 7.5. The experiments were performed with 100 uM GST-TcPINK1 (143-570) in the cell and 3 mM AMP-PNP in the syringe. Both the protein and the ligand had been buffer-exchanged into the ITC buffer prior to the experiment. The measurements were made at a constant temperature of 25 °C using the ITC200 calorimeter (Malvern). The data was analyzed using Origin software (version 7). The stoichiometry was fixed to 1.

2.3.2 ITC experiments of Parkin R0RBR

ITC measurements were carried out at a constant temperature of 20°C using ITC200 (Malvern). Samples were in 50 mM Tris–HCl pH 7.4, 150 mM NaCl, 1 mM TCEP. Data were analyzed using Origin v7 software. Protein concentrations in the cell and syringe are indicated in the figures. The stoichiometry was determined experimentally for Ubl and pUb titrations and

generally refined to values between 0.8 and 1.0 (Sauve et al., 2015). The stoichiometry was fixed to 1:1 for UbcH7 titrations

2.4 NMR titration experiments

2.4.1 NMR titration experiments for TcPINK1 and Ubl

^{15}N-labelled UbL and unlabeled GST-TcPINK1 (121-570) were buffer-exchanged into NMR buffer (50 mM Tris, 100 mM NaCl and 1mM DTT pH: 7.5). Experiments were performed using a 600 MHz NMR spectrometer (Bruker) equipped with a room-temperature triple-resonance probe, at a temperature of 295 K. 5% D_2O was added to each sample for for the lock signal. Titrations were then performed with GST-TcPINK1 (121-570) and 200uM ^{15}N-UbL at 1:2, 1:4 and 1:8 molar ratios. ^{1}H -^{15}N sensitivity-enhanced HSQC spectra were acquired at each titration point, as well as a reference spectrum with 200 μM ^{15}N-UbL. Experiments were done with 64 scans per titration point. All spectra were contoured to the same level. The data was processed using NMRView and visualized using Sparky. The NMR assignments for UbL were obtained from Trempe *et al*. 2009 and mapped onto the HSQC spectra. Intensities for individual peaks (corresponding to each amide) were obtained from each spectra and represented as a ratio of the respective intensity in the reference spectrum (Ubl alone). Protskin (Gehring Lab) was used to map the intensity ratios (corresponding to the 1:8 titration point) onto the UbL structure (from Trempe *et al*. 2009). The results were visualized in Pymol. The results were used to guide the mutagenesis of the UbL domain for phosphorylation assays.

2.4.2 NMR experiment for R0RBR binding with pUb

^{1}H -^{15}N HSQC spectra were collected for 0.2 mM ^{15}N-Ubl alone and following the addition of unlabeled Parkin R0RBR, or Parkin R0RBR and pUb at equimolar concentrations. Prior to the experiment all proteins had been exchanged into NMR buffer (20 mM Tris-HCl, 120 mM NaCl, and 2 mM DTT pH 7.4). The spectra were acquired on a Varian NMR spectrometer at a field strength of 800 MHz at a temperature of 293 K, processed using NMRpipe and analyzed using NMRView J.

2.5 Small-angle X-ray scattering (SAXS)

Small-angle X-ray scattering data was collected on the SIBYLS beamline (12.3.1) at the Advanced Light source (Lawrence Berkeley National Laboratory). Data was collected for 0.5 or 1 s at 20 °C, at protein concentrations of 2, 4 and 8 mg/ml for L266K Parkin and 1.5, 3 and 6 mg/ml for WT Parkin. Background scattering from the buffer (50 mM Tris-HCl pH 8.0, 150 mM NaCl, 2% glycerol and 10 mM DTT) was measured for 0.5 - 1 s. Scaling, buffer subtraction, and merging were performed using the ATSAS software suite (Petoukhov et al., 2012). Pairwise distance distributions were calculated using GNOM.

2.6 Multiple-angle light scattering (MALS)

Data were collected with a miniDAWN Treos (MALS) and an OptiLab rEX (refractive index) instruments (Wyatt Technology Corporation), connected to a Waters AllianceBIO HPLC with autosampler fitted with a Superdex 200 Increase analytical gel filtration column (GE). The column was equilibrated in 50 mM Tris/HCl, 300 mM NaCl, 1 mM DTT, pH 8.0 and all experiments were performed at room temperature. Fifty (50) μL of protein solution (previously centrifuged) was injected per run, and resolved on-column at a flow rate of 0.5 mL/min. Three-angle MALS data and refractive index were collected with a 1 Hz sampling rate. Data were analyzed with the software Astra (Wyatt). Peaks were identified with UV and the molecular weights derived from light scattering data normalized with concentrations derived from the refractive index.

Chapter 3. PINK1 expression and purification

3.1 Expression of Human PINK1

Performing structural studies on proteins such as NMR and X-ray crystallography requires large quantities (on the order of milligrams) of stable and pure proteins. Functional experiments including protein-protein or protein-ligand binding assays such as ITC also requires similar amounts of proteins. To obtain large amounts of proteins, bacterial expression systems or Insect cell lines (infected with baculovirus) are commonly used. The latter is advantageous over the former in the sense that it provides eukaryotic machinery for the protein folding and post-translational modifications. However, the method is method is expensive, difficult to maintain and the time required to get to purified desired product in greater. For these reasons we chose to start with a bacterial expression to obtain human PINK1 for structural studies.

Human PINK1 kinase domain (residue 148-511) and kinase domain and C-terminal region constructs (residue 148-581) cloned in pGEX-6p1 vectors were expressed as GST fusion proteins and purified. Lysis of cells was performed in the presence of protease inhibitors. The GST tag was cleaved off using the 3C rhinovirus protease overnight. GST-tag cleavage also serves as a diagnostic for the successful purification of the desired protein. To take into account any changes in the stability of the protein at 4^{o}C overnight, control samples were also frozen at -80^{o}C. The samples were loaded on SDS-PAGE gel and are shown in Figure 3.1. Upon addition of 3C, both GST fusion proteins (73 and 66 kDa bands) lose GST (26kDa band) and yield non-fusion forms (47 and 41 kDa bands) showing that the desired protein is present in the sample. However for both proteins, the gel results also shows two undesirable features: degradation and the presence of impurities. The former is visible in the form of a ladder-like pattern of bands above 26 kDa in size (in all samples without 3C) that goes away upon the addition upon the addition of 3C protease. This implies that these bands correspond to GST fusion proteins (and hence truncated forms of PINK1) degraded by endogenous proteases in E.coli at different positions following the GST tag. The impurities are visible in the form of extra bands present around 65kDa and 75kDa (close to both GST fusion forms). Since the proteins are present in both samples and do not show a shift upon 3C addition, it is clear that they are not GST forms

of PINK1. They likely correspond to bacterial chaperones that bind to PINK1 and coelute with it. Indeed, the bacterial chaperone GroEL (~60 kDa) has been reported to copurify with unstable GST-fusion proteins (Rohman and Harrison-Lavoie, 2000). There is also no visible difference between the protein samples stored at -80^{o}C and 4^{o}C on gel; no precipitation was observed at 4^{o}C either. Including impurities and degraded product, the yield of human PINK1 from 1 liter E.coli cultures was found to be no greater than 1 mg. Though some studies reported the purification of different constructs human PINK1 from E.coli, the purification yields have not been reported (Sim et al., 2006, Beilina et al., 2005, Silvestri et al., 2005, Woodroof et al., 2011). One of these studies also reports the poor solubility of full length human PINK1 and toxicity to E.coli (Beilina et al., 2005) and another one reports endogenous degradation of the 121-581 construct (Sim et al., 2006). As a result, many groups have considered Baculovirus infected insect cell lines (Sf9) as alternative expression systems for human PINK1 (Sim et al., 2006, Woodroof et al., 2011, Hertz et al., 2013). Notably, one study found that co-expression with the mitochondrial chaperone TRAP1 in Sf9 cells dramatically increases the expression of human PINK1 [6]. We therefore tried the co-expression of human PINK1 with TRAP1 in E.coli (Pridgeon et al., 2007, Hertz et al., 2013), as well as the use of denatured E.coli lysate and ATP to remove the GroEL impurity (Rohman and Harrison-Lavoie, 2000). However the problem of protein degradation and co purification with chaperones persisted (data not shown). We therefore conclude that because of its endogenous degradation in E.coli and copurification with chaperones, human PINK1 is unstable (does not fold well) and unfit for expression in E.coli. We therefore turned our attention towards orthologs of human PINK1.

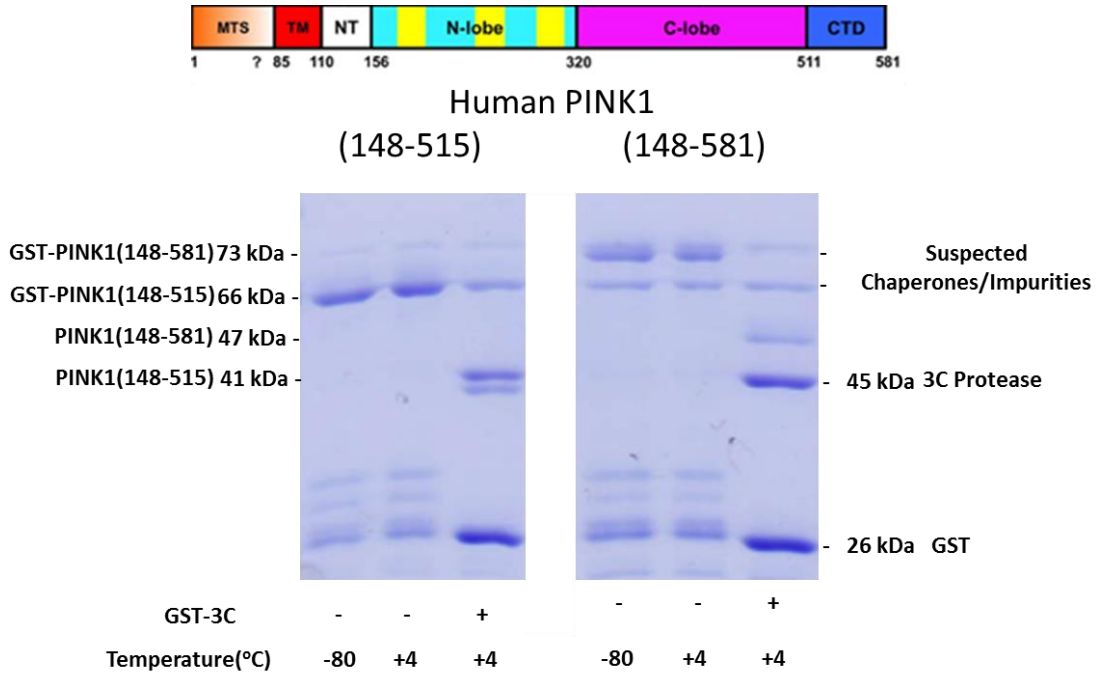

Figure 3.1 **Expression of Human PINK1** (above) Schematic representing the domain organization of PINK1 and SDS-PAGE gels from the purification and 3C cleavage of (below, left) kinase domain (below, right) kinase domain and C-terminal region.

3.2 Expression of TcPINK1

In 2010, a study reported that recombinant expressed PINK1 from the insect species *Pediculus humanus corporis* (common louse) and *Tribolium castaneum* (figure 3.2 A) (TcPINK1) displayed much higher kinase activity than human PINK1 and drosophila PINK1, with TcPINK1 showing the greatest levels of activity towards generic substrates including histone H1 and the myelin basic protein (Woodroof et al., 2011). Though this study used E.coli expression lines for the study, the yields of purification were not reported. We performed pairwise sequence alignments between human PINK1 and TcPINK1, and found that the full-length forms of the two proteins have a sequence identity of 33% while the kinase domains is about 40% identical. At this level of conservation of sequence, the tertiary structure and the fold of the protein is usually conserved (Gong et al., 2009). In particular, the architecture of kinase domains is generally conserved across all kinases (Kornev and Taylor, 2010). The multiple sequence alignment (Figure 1.4) indicates that the active site residues are conserved as well. One major difference between the kinase domain of human PINK1 and TcPINK1 is that the latter has a much shorter insert 1. Taking the increased activity and high sequence homology of TcPINK1 into account, we hypothesized that TcPINK1 might be a suitable model for human PINK1 for

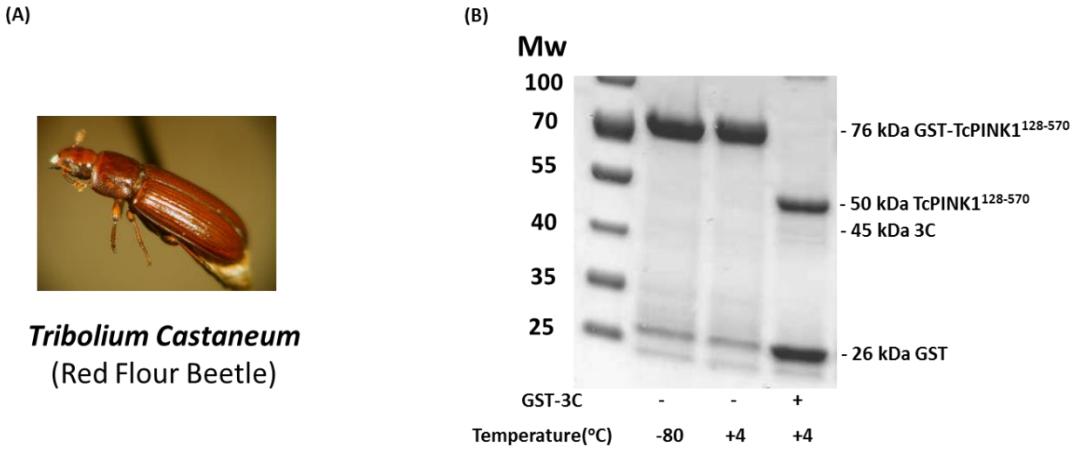

Figure 3.2 **Expression of TcPINK1** (A) Tribolium Castaneum (B) SDS-PAGE showing purified TcPINK1 (128-570) before and after 3C cleavage with the molecular standards and theoretical molecular weight of the proteins

structural and functional studies. Therefore, the open-reading frame for TcPINK1 with codon-optimization for E.coli was cloned in the pGEX-6p1 vector and for expression in E.coli and purification. Figure 3.2 shows the SDS-PAGE for the elution and 3C cleavage of TcPINK1 (128-570), a construct that starts within the NT linker and includes the kinase domain and C-terminal region. In contrast to human PINK1, TcPINK1 shows almost no degradation nor co purification with impurities, and 3C cleavage generates a stable 50 kDa protein. Different constructs of TcPINK1 (1-570), (121-570) and (143-570) have since been purified successfully with similar observations. Subsequently, bacterial growth media was changed from LB to TB (Terrific broth) to improve protein yield. Lysis buffer composition has been optimized to improve protein yield and stability. These optimizations include the addition of lysozyme, changing pH from 7.5 to 8.0 and increasing salt concentration from 100 mM to 300 mM. It was also found that the addition of 0.1% CHAPS to the elution buffer helped increasing its solubility and preventing precipitation upon concentration. Section 2.1.1 contains the final optimized purification protocol. With this optimized protocol the average yield of pure fusion protein from 1 Liter cultures is around 40 mg.

3.3 Deletion of Insert1 from human PINK1

Knowing that TcPINK1 expresses well, we wished to explore the differences between human PINK1 and TcPINK1 that enable the latter to express well in bacterial expression systems. As mentioned previously, TcPINK1 differs from human PINK1 in that it has a shorter

insert 1. In human PINK1, insert 1 is composed of 30 amino acid spanning residue 181 through residue 210. While no structural information is available for this region, it is likely to form an unstructured loop because it is rich in glycine and proline residues. We hypothesized that the difference between TcPINK1 and human PINK1 expression arises because of this loop, which in the case of human PINK1 makes the protein prone to endogenous degradation by proteases or affects its folding in E.coli. Using site-directed mutagenesis, two different lengths of insert 1 were deleted from human PINK1 (148-581) to generate Δ184-206 or Δ181-209 constructs and expressed in E.coli. The SDS-PAGE analysis (figure 3.3) indicates that either of the proteins, just like WT (148-581), co-purify with impurities, are significantly degraded and have low proportion of non-degraded protein of interest (compared to the impurities). Samples of Δ184-206 contain lesser degraded protein than WT, but more than Δ181-209. This observations suggests that insert1 might indeed be the target for endogenous proteolytic cleavage in E.coli. However, the solubility of both constructs lacking the insert was poor. The appearance of the band close to 66 kDa (as in figure 3.1) suggests the presence of chaperones and alludes towards the instability of each protein. Including degraded protein and chaperones the total yield form 1 Liter cultures of E.coli was 0.5 mg (as measured by Bradford assay). From this experiment it can be concluded that the inability to express human PINK1 cannot be attributed solely to insert 1, and other differences between the TcPINK1 and human PINK1 sequences must contribute.

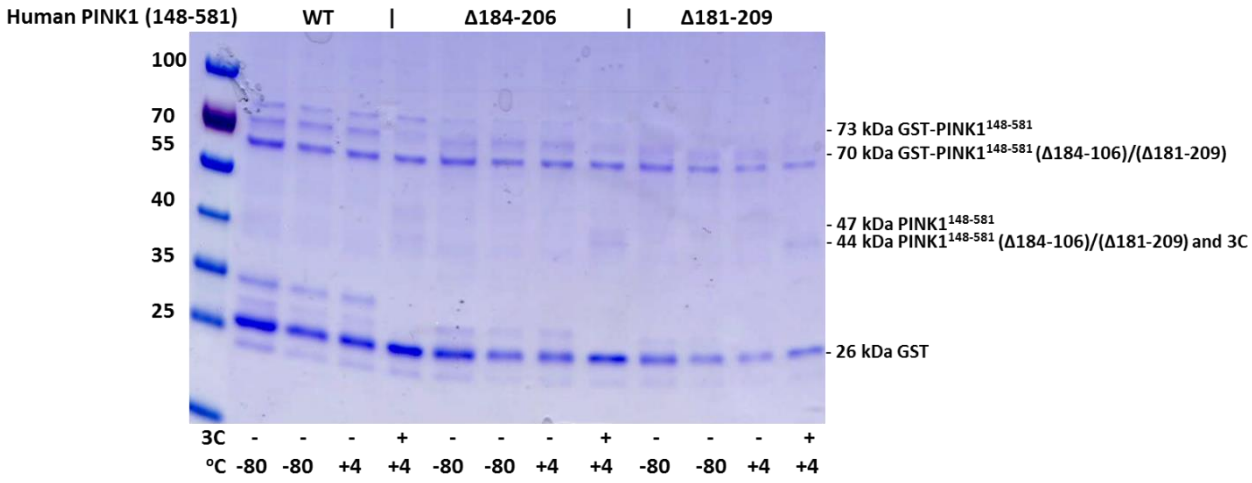

Figure 3.3 **Deletion of Insert 1 from human PINK1** Two different lengths of insert 1 were deleted from human PINK1 (148-581), expressed and purified from E.coli. The samples at -80 °C correspond to elutions concentrated before and after concentration (same amounts loaded).

3.4 Expression of C-terminal region of PINK1 and TcPINK1 kinase domain

The C-terminal region of PINK1 (511-581) is not known to share homology with any known protein. Reports have suggested that it contains alpha helices, has inhibitory (Woodroof et al., 2011, Silvestri et al., 2005) or activating roles for the kinase activity of PINK1, and also is also involved in substrate recognition (Sim et al., 2006). Since this region is not shared in homology with the kinase domain of CamKII (as mentioned in the introduction), we hypothesized that it might be an independently folding domain and hence can be expressed in E.coli independently from the rest of the protein. Since this region is short, it could also be a good target for NMR studies. This putative domain spans residues 511-581 in human PINK1 and residues 486-570 in TcPINK1. Both were cloned in pGEX-6p1 and expressed in E.coli. Figure 3.4 (A) shows that the expression of TcPINK1 C-terminal is negligible since the GST-fusion form of the protein is not visible. Since GST is visible, the C-terminal region probably got cleaved inside cells and did not elute. While bands are observed at the expected size for human PINK1 C-terminal region in GST-fusion form, they do not undergo any change upon addition of 3C protease indicating they are either impurities or aggregated GST-fusion forms. The results led us to conclude that the C-terminal region of PINK1 is not an independently folding domain and relies on the kinase domain for its folding (in the case of TcPINK1).

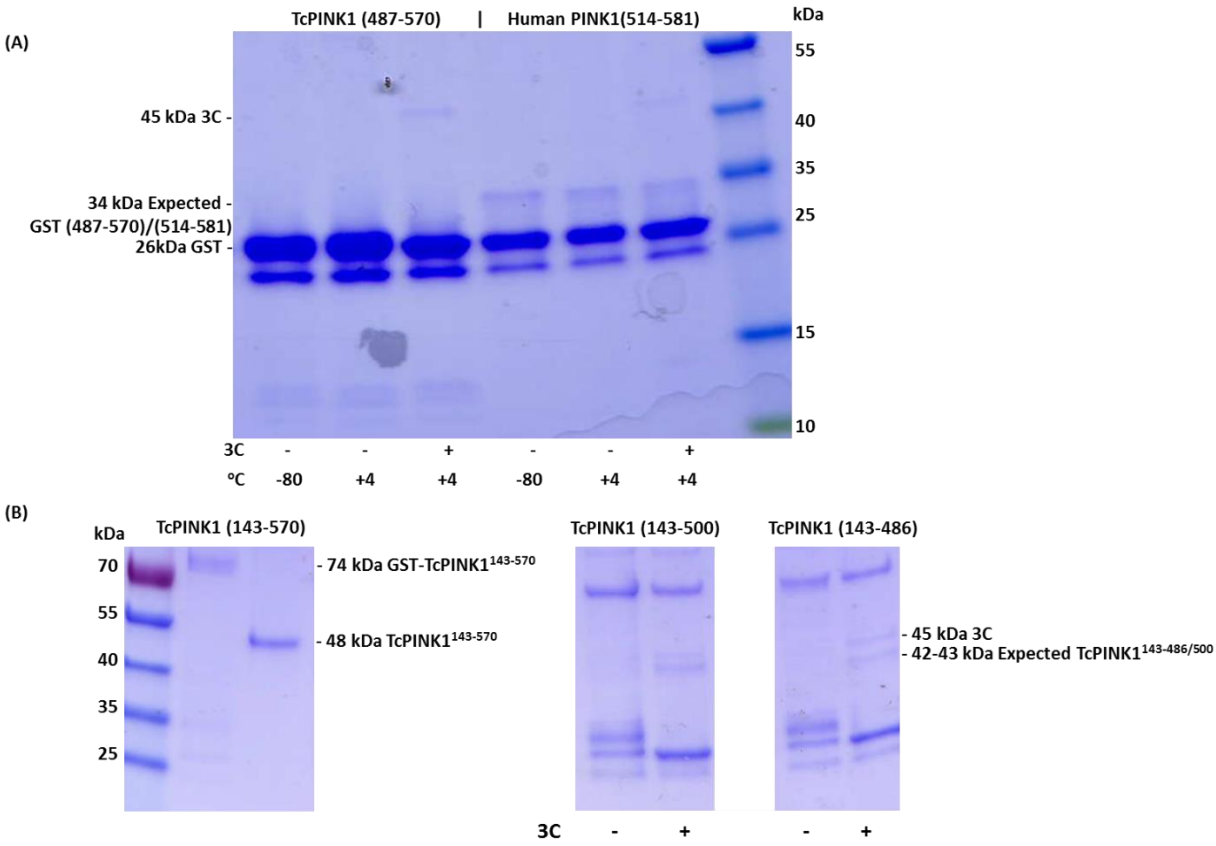

Figure 3.4 **Expression of C-terminal region of PINK1 and kinase domain of TcPINK1** (A) expression tests on TcPINK1 and human PINK1 C-terminal region. (B) Expression of TcPINK1 (143-570), (143-486) and (143-500); all images in (B) were cropped from the same gel image.

In order to investigate the effect of deleting the C-terminal region of TcPINK1 on its kinase activity, TcPINK1 (143-486) and TcPINK1 (143-500) were expressed in E.coli (Figure 3.4 B). As opposed to TcPINK1 (143-570), the constructs from which C-terminal region was deleted did not purify well, and similar to human PINK1 kinase domain construct (Figure 3.1), the elutions contain mostly degraded protein and impurities. Taken together, these results imply that the C-terminal region is an integral part for the kinase domain and both depend on each other for proper folding. Hence the C-terminal region should not be classified as a domain.

3.5 Expression tests on other PINK1 orthologs

Besides TcPINK1, we also considered cloning and expressing other orthologs of PINK1. The intent behind this exercise is to identify candidate(s) most suitable for crystallization. We expressed PINK1 constructs (following the transmembrane region) from *Gallus gallus* (chicken), *Camponotus floridanus* (ant), *Pediculus humanus corporis* (louse), *Dendroctonus penderosae*

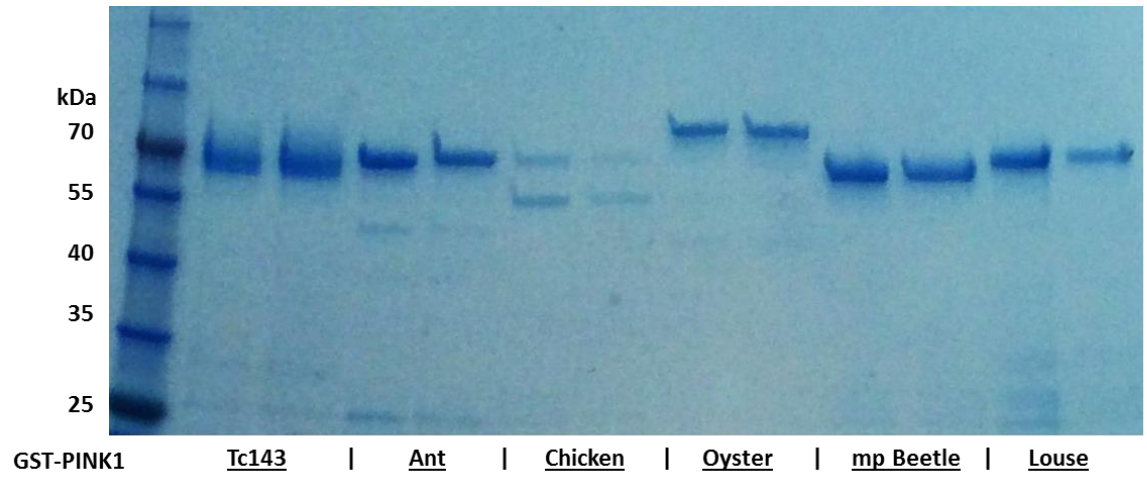

Figure 3.5 **Small-scale expression of PINK1 orthologs.**

(mountain pine beetle) and *Crassostrea gigas* (Oyster). Owing to the success with TcPINK1, more insect species were considered for expression in E.coli than other vertebrate species. The expressed constructs were cultured on a small-scale (15 ml bacterial cultures) and purified as GST fusion proteins. Figure 3.5 is an SDS-PAGE gel showing the elutions of these proteins. All proteins show a band close to 70 kDa on gel. The amount of protein eluted for GST-Chicken PINK1 is lesser compared to the rest and it also gives a degraded product close to 55 kDa. All the other proteins show almost no degradation or impurities. Oyster PINK1 travels higher on gel compared to the rest of the proteins and also showed aggregation in solution. Drosophila and mouse PINK1 were not found to express well in E.coli (not shown). Of these constructs, both ant and beetle PINK1 appear the most stable; unsurprisingly, these orthologs have the highest sequence identity with TcPINK1.

3.6 Size-exclusion Chromatography studies of TcPINK1

Studies conducted thus far on PINK1 have focused almost exclusively on PINK1's functional role. Not only is there a lack of experimental structures for PINK1, there are also no studies reporting the behavior of PINK1 in solution in terms of its oligomeric state. In 2013, using PINK1 tagged with multiple fluorophores analyzed by native PAGE gels, a study reported that PINK1 might exist as a dimer on mitochondria in complex with TOM in a mitochondrial damage-dependent manner (Okatsu et al., 2013). Since the same group earlier reported that PINK1 auto phosphorylates in trans (Okatsu et al., 2012), it was suggested that dimerization is

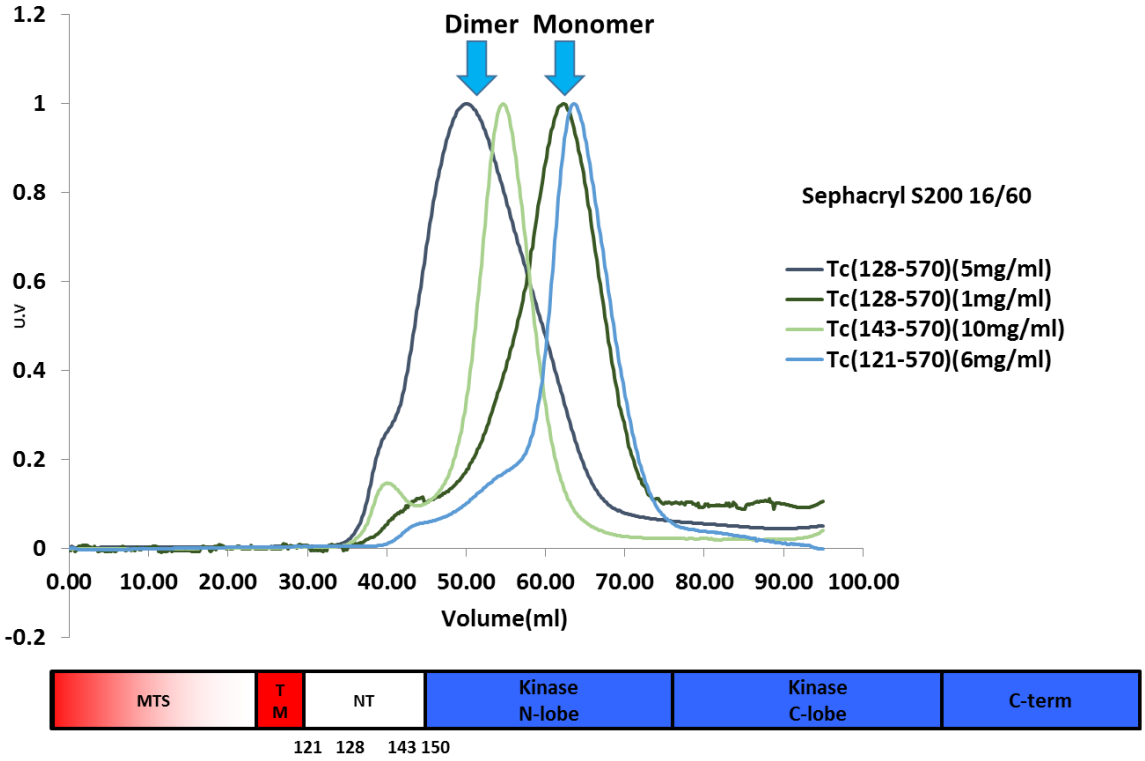

Figure 3.6 **Size-exclusion study of TcPINK1 constructs using Sephacryl S200** (Above) Sephacryl S200 16/60 profiles of different TcPINK1 constructs at different concentration. The peak intensities for all profiles were normalized to bring them to the same height. (Below) Schematic representing the positions of residues 121, 128 and 143 in TcPINK1.

an essential requirement for autophosphorylation and activation of PINK1. Nonetheless, there are still no studies about the region in PINK1 that is responsible for mediating dimerization. Size-exclusion chromatography using Sephacryl S200 column was performed with different concentrations of different constructs of TcPINK1 (Figure 3.6). We used GST as a standard for this column and found it to elute at 65ml (not shown). Since GST forms dimer in solution, this elution volume corresponds to a 52 kDa mass (2 x 26 kDa). TcPINK1 (128-570) was injected at 1 mg/ml (low concentration) and 5 mg/ml (higher concentration) on column. Surprisingly, at low concentration the TcPINK1 (128-570) elutes close to 65 ml (close to monomer) and at higher concentration it elutes at 45 ml. The latter probably corresponds to a trimer or higher oligomeric forms since IgG (a 160 kDa protein) elutes at a similar volume according to the column manufacturer datasheet. This implies that this construct of TcPINK1 undergoes concentration-dependent oligomerization. The peaks for both samples are also skewed and broad, alluding to the presence of multiple forms of TcPINK1 (monomer or oligomer). TcPINK1 (121-570) (which starts right after the transmembrane helix) elutes at 67 ml when injected at a

concentration of 6 mg/ml (higher concentration) and is most likely a monomer, while TcPINK1 (143-570) elutes at about 53ml when injected at a concentration of 10 mg/ml. According to manufacturer's instructions, bovine serum albumin (a 67 kDa protein) elutes between 55 and 60ml from this column under similar conditions. Hence TcPINK1 (143-570) is most likely a dimer at this concentration. The peaks for both TcPINK1 (121-570) and TcPINK1 (143-570) are also sharper compared to TcPINK1 (128-570) pointing towards a greater homogeneity of species in solution. To confirm these findings, we performed higher resolution size-exclusion chromatography using an analytical Superdex 200 Increase column in combination with multiple-angle light scattering (MALS) on TcPINK1 (121-570) and TcPINK1 (143-570). MALS allows the determination of the molecular weight of eluting species independently of their shape in solution and hence can be used confirm the oligomeric state of different species. Both proteins were investigated at 3 mg/ml and 6 mg/ml concentrations. Figure 3.7 (A) shows that the TcPINK1 (143-570) peaks elute earlier compared to TcPINK1 (121-570) consistent with the observation form the Figure 3.6. TcPINK1 (121-570) samples also show minor peaks close to the elution time of TcPINK1 (143-570) that possibly corresponds to a small proportion of dimer in solution. For both proteins some concentration-dependent changes are observed in the elution profile: both proteins shows small shift towards the right upon decrease the concentration from 6 to 3 mg/ml. The molecular weights corresponding to the major peaks for each sample were estimated using MALS (Figure 3.7 B). As shown, at lower concentration TcPINK1 (121-570) is monomeric but the shift of average mass from 51 kDa to 56.1 kDa at 6 mg/ml shows at least a small proportion of dimer is present in solution. Similarly TcPINK1 (143-570) is dimeric at 6mg/ml and the decrease in concentration causes decrease the average mass, showing that a small proportion of the protein is monomeric at lower concentration.

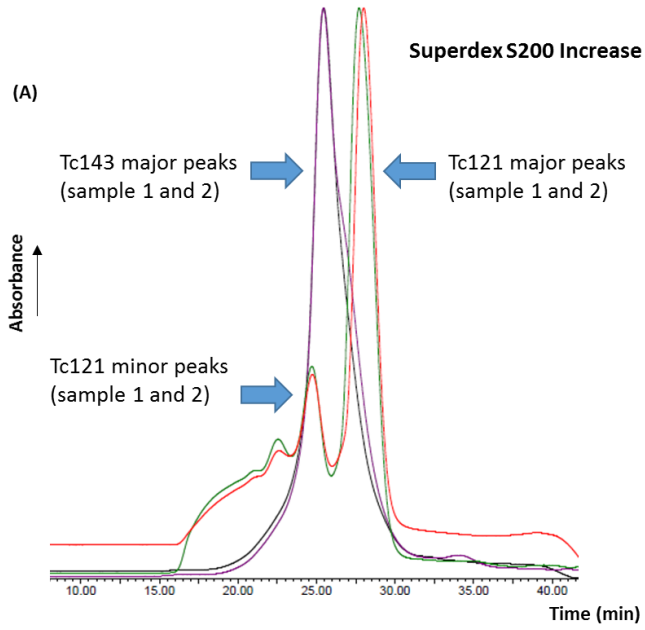

(B) **MALS Calculations**

Sample	Theoretical M.W.	Measured M.W of Major peak
Tc121(sample1) (**3 mg/ml**)	51.1 kDa	51.7 kDa
Tc121(sample2) (**6 mg/ml**)	51.1 kDa	56.1 kDa
Tc143(sample1) (**3 mg/ml**)	48.1 kDa	80.0 kDa
Tc143(sample2) **(6 mg/ml)**	48.1 kDa	87.0 kDa

Figure 3.7 **SEC-MALS study of TcPINK1** (A) Superdex S200 increase profiles of TcPINK1 (121-570) (green: 3 mg/ml, red: 6mg/ml) and TcPINK1 (143-570) (blue: 3 mg/ml, black: 6 mg/ml) (B) Mass estimation based on MALS for the major peaks.

These comparisons indicate that TcPINK1 can undergo variable levels of concentration-dependent dimerization depending on the length of N-terminal linker in the construct; 121-570, that contains the entire length of the NT region and stays mostly monomeric in solution even at higher concentration while the 143-570 construct is mostly dimeric even at lower concentration. The 128-570 construct is the intermediate case in the sense that it undergoes shifts from monomer to dimer (on average) upon similar increases in concentration, though the peaks are broader than either of the other constructs. It is hence likely that the NT region regulates the oligomerization of PINK1 in solution. Despite the evidence of dimerization in cells (Okatsu et al., 2013) it is not clear if this phenomenon is physiologically relevant. PINK1 localizes on the OMM in complex with TOM in its full-length form so it will be important to investigate the oligomeric state of full-length TcPINK1 in solution. It can be speculated that 121-570 and 143-570 represent two different forms of PINK1 in the cells; in the former case might correspond to a conformation of NT linker folding back to interact with the kinase domain and prevent its dimerization (in the cytoplasm) while in the latter case the association with TOM subunits might product a conformational change that changes the position of the NT and allows the dimerization of adjacent kinase domains.

Chapter 4. PINK1 Kinase Activity

4.1 TcPINK1 phosphorylates Ub *in vitro*

As described in the introduction chapter, PINK1 was discovered to be a kinase of ubiquitin and Parkin. I have also described in the previous chapter that by virtue of its close homology with human PINK1, TcPINK1 is likely to conserve most structural elements that convey selectivity for ubiquitin Ser65. Based on conservation one can also hypothesize that TcPINK1 will also be functionally similar to Human PINK1. We tested this hypothesis by investigating the ability of TcPINK1 to phosphorylate ubiquitin *in vitro* (Figure 4.1). The phosphorylation was analyzed loading the reaction on regular and phos-tag SDS PAGE gels. Compared to the regular SDS-PAGE gel (figure 4.1 (A), bottom panel), the His-ubiquitin band is shifted upward in a TcPINK1-dependant manner (figure 4.1 (A), top panel), indicating that TcPINK1 had phosphorylated His-Ub. In order to confirm these finding, we performed similar phosphorylation assays with and without ATP and inspected changes in intact Ub with MALDI-TOF mass spectrometry. The resulting spectra (corresponding to singly charged species) are shown in Figure 4.1 (B). The spectrum corresponding to the reaction with ATP (top panel) contains an extra peak at about 8648 Da which is ~ 80 Da greater in mass compared to the Ub peak (8568 Da), but this change was not observed in the reaction without ATP (bottom panel) . The mass increase corresponds to the incorporation of a phosphate group to Ub. The extent of phosphorylation is lesser as observed with MALDI-TOF compared to the Phos-tag gel. This can be attributed to the fact that phosphate groups are labile and can dissociate upon MALDI laser irradiation. Ubiquitin is entirely conserved across all species and shares the Ser65 residue with Parkin Ubl (besides other residues), which has been reported as a phosphorylation site target site for PINK1. We hypothesized that owing to the high degree of similarity between Ub and Parkin UbL, this phosphorylation is likely to occur at Ser65 on Ub as well. As expected, S65A Ub did not show a shift on Phos-tag gel (figure 4.1 (A), top panel). The results suggest Ub phosphorylation is conserved in insect species such as TcPINK1 and that phos-tag is a reliable assay for detecting Ub phosphorylation. Our results are in concurrence with other studies that showed TcPINK1 can phosphorylate Ub (Kazlauskaite et al., 2014, Kane et al., 2014).

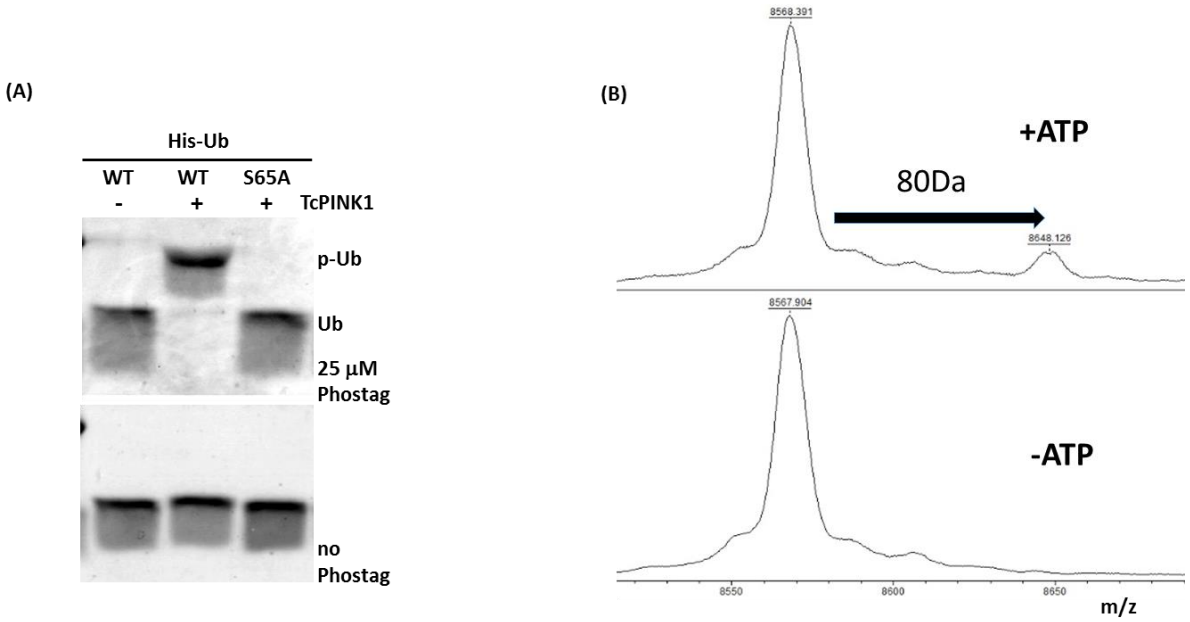

Figure 4.1 **TcPINK1 can phosphorylate Ub *in vitro*** (A) phosphorylation assay with WT or S65A His-Ub and GST-TcPINK1 (128-570) loaded on regular or Phos-tag gel (15% Tris Glycine). This result was contributed to (Koyano et al., 2014). (B) MALDI-TOF spectra of Ub phosphorylation reactions with or without ATP. The labelled value for each peak represents the m/z (mass to charge) value for singly charged species. Note: These experiments were performed before the first reports about Ub phosphorylation by PINK1 (Kazlauskaite et al., 2014, Kane et al., 2014) were published.

4.2 UbL phosphorylation by TcPINK1

Phosphorylation of full-length human Parkin or its Ubl domain on Ser65 has been previously reported by Muqit and co-workers, which was shown to be responsible for Parkin's activation (Kondapalli et al., 2012). I used the Ubl domain from Rat Parkin as a substrate for TcPINK1 since there are a greater number of structural studies available for this domain (Trempe et al., 2009, Trempe et al., 2013) and it also has been proposed to have a higher solubility. Human Parkin UbL domain is very similar to its Rat ortholog with only 3 amino acid substitutions including Trp74, which is a glutamine in Rat and potentially increases the solubility (Trempe et al., 2009). Work in my lab has shown that Ubl domain of TcParkin does not express well in E.coli (data not shown), so it was not considered further for this analysis. The results indicate that Rat Ubl gets phosphorylated by TcPINK1 (Figure 4.2).

4.3 NT truncations of TcPINK1 does not affect kinase activity

In the previous chapter, it was shown that the NT region (121-156) might play a role in regulating the oligomeric state of the protein as TcPINK1 (121-570) was found to be mostly a

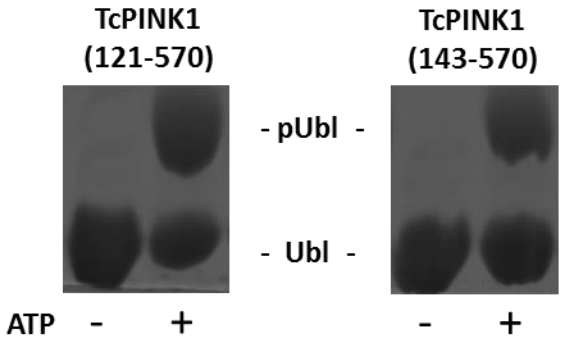

Figure 4.2 **Ubl Phosphorylation by different TcPINK1 constructs** Ubl phosphorylation assays conducted with TcPINK1 (121-570) or TcPINK1 (143-570) under the same conditions.

monomer in solution whereas TcPINK1 (143-570) was found to be mostly dimeric. However is it not understood if this region has any impact on the activity of PINK1. I asked whether the NT region of the protein is likely to regulate its kinase activity. Figure 4.2 shows that both constructs are active in terms of Ubl phosphorylation. Therefore the NT region is not likely to interfere with the activity of the kinase domain.

4.4 PINK1 Enzyme Kinetics

In order to investigate the difference between the phosphorylation of Ub and Ubl by PINK1, a Michealis-Menten kinetics approach was taken. Michealis-Menten analysis provides two key parameters for enzymatic reactions: K_m, that provides a measure of substrate affinity for the enzyme, and k_{cat}, that gives an estimate of the catalytic turn-over of a reaction. Both of these parameters are specific to every enzyme-substrate reaction and can used to understand the difference in activities for different substrates or rationalize the effect of mutations in enzymes. In order to do so, time course kinase reactions were performed with fixed concentration of His-Ub and TcPINK1 to find out the time points, which are within the bounds of the initial reaction rate i.e. a linear increase in phosphorylation of Ub over time (Figure 4.3). These time points can then be used to find the initial rate of reaction for different concentrations of substrate which when plotted out can be used to give estimates of K_m and V_{max} (maximum rate). Figure 4.3 A and B indicate that Ub phosphorylation increases linearly over time until the first five minutes of the reaction, but since the 10min time point does not lie close to the linear line, the effects of the reverse reaction start becoming prominent after the 5 min time point. For Ubl phosphorylation time course (Figure 4.3 C and D), the product

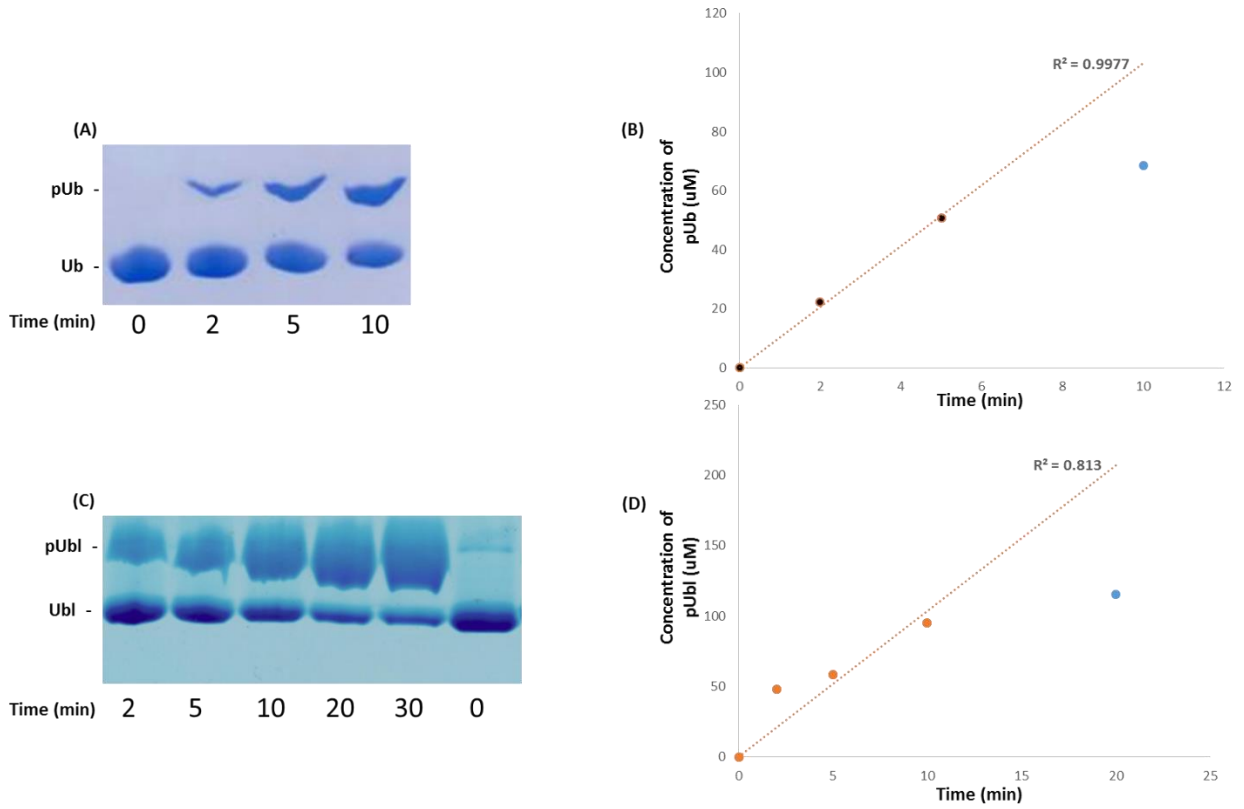

Figure 4.3 **Ub and Ubl phosphorylation time course kinase assays** (A) His-Ub time course assay and (B) corresponding graph. (C) Ubl time course assay and its corresponding graph. The graphs were obtained following background subtraction and normalization of intensity counts with respect to concentration. Data points not following the linear trend in each graph are labelled with blue dots. R-squared values for the fit of the data to the linear line are stated.

formation trajectory is linear uptil the 10 min time point but not afterwards. Hence for both Ubl and Ub phosphorylation reactions at different substrate concentrations, the 5 min time point can be used as the time corresponding to the initial rate of reaction.

Kinetics experiments were then performed using a fixed time point (5min) and different concentrations of Ub or Ubl. Following densitometry of the phosphorylated protein, the results were plotted and fitted to the Michealis-Menten equation to calculate the values of K_m and V_{max} (Figure 4.4). The results indicate that TcPINK1 has a 10 times more favorable K_m for Ubl (Figure 4.4 B and E) compared to Ub (Figure 4.4 A and D), which indicates a greater affinity of the enzyme for the Ubl domain than Ub. However the catalytic turnover rate k_{cat} (V_{max}/[Enzyme]) are 2 times greater for Ub. This could imply that though binding of Ubl to TcPINK1 is more favorable than Ub, once bound the conversion of Ub to pUb is faster than Ubl. Moreover, the uncertainty on k_{cat} is probably greater than determined from the curve-fitting procedure;

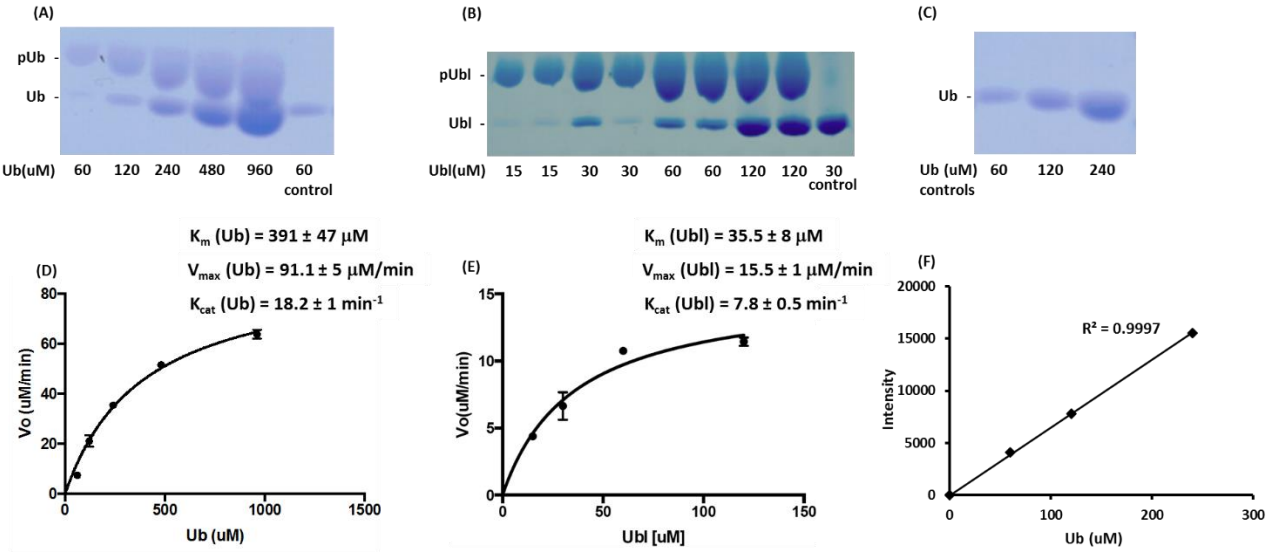

Figure 4.4 **Michealis-Menten modelling of Ub and Ubl phosphorylation Kinetics** 5 minute phosphorylation reactions for (A) His-Ub and (B) Ubl and their corresponding graphs (D) and (E) (background subtracted and normalized with respect to concentration and time). The graphs in (D) and (E) are global fits to data collected for 2 sets of reactions for both Ubl and His-Ub performed independently. Only one set of reactions for Ub is displayed (A). (C) Control Ub samples loaded on phos-tag gel and (F) analyzed by densitometry.

systematic errors such as pipetting of enzyme dilutions will increase the uncertainty in the measurements. Thus, the difference in k_{cat} is likely insignificant, whereas the difference in Km is marked and insensitive to the enzyme concentration estimation. The catalytic efficiency (k_{cat}/K_m ratio) is significantly greater for Ubl (~0.22) compared to Ub (~0.05), which implies that both kinetically and thermodynamically Ubl might be preferred as a substrate over Ub by TcPINK1. The findings need to be established for human PINK1.

In order to ensure that the kinetic data observed was purely due to Ub or Ubl phosphorylation and not because of a non-linear protein staining by Coomassie, control samples (unphosphorylated) of Ub and Ubl were run on phos-tag gels and the relationship between signal intensity and concentration was observed using graphs. This is particularly important for small proteins like Ub and Ubl for which poor reactivity with Coomassie can cause staining anomalies. The results for Ub is shown as an example in Figure 4.4 (E and F) as an example. The results indicate unphosphorylated Ub gives a perfectly linear increase in intensity with concentration. Hence the kinetic data observed is reliable.

In order to characterize PINK1 further, similar kinetic analysis was performed for calculating K_m of TcPINK1 for ATP by observing Ub phosphorylation as a function of ATP concentration. The

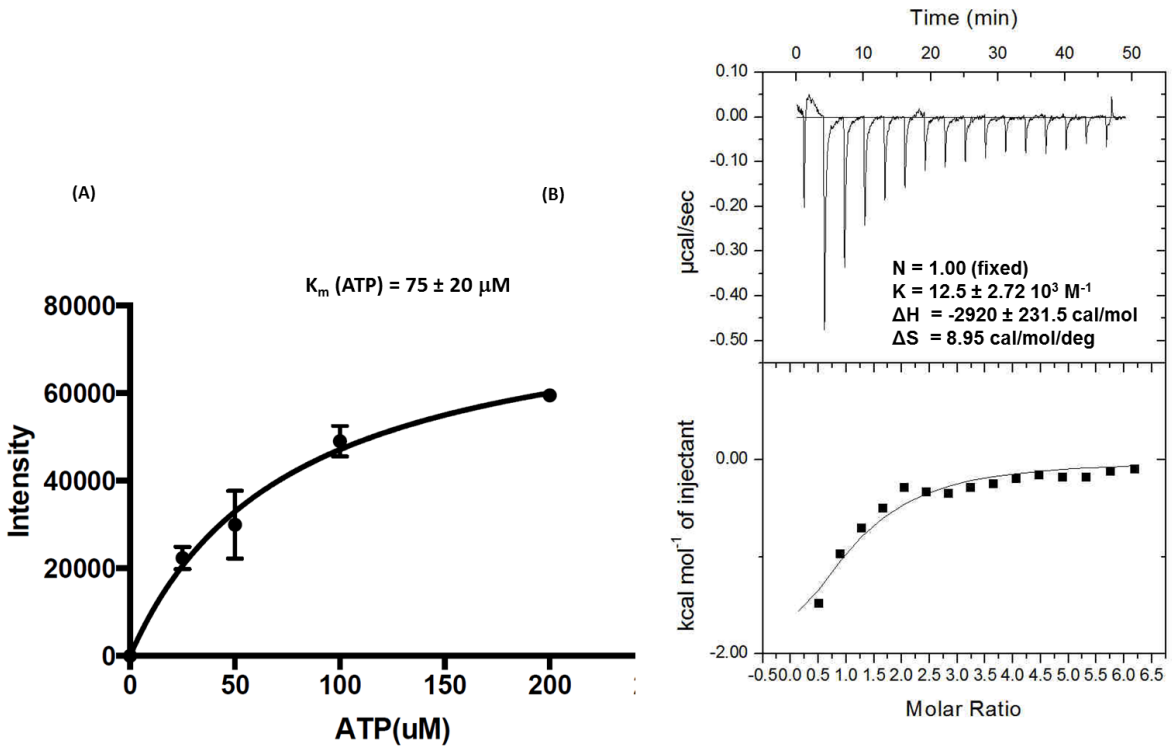

Figure 4.5 **Kinetic and Binding experiments between TcPINK1 and ATP** (A) Graph for His-Ub phosphorylation reactions plotted against ATP concentrations and the value of K_m calculated from Michealis-Menten modelling. (B) ITC experiment for the binding between AMP-PNP and GST-TcPINK1 (143-570) and the obtained values for thermodynamic parameters. The stoichiometry (N) was fixed to 1.0.

reactions were performed with an excess of Ub but with ATP as the limiting substrate. The result following the Michealis-Menten modelling of the data are shown in Figure 4.5 (A) and show that K_m is about 75 μM. This result is very similar to the reported K_m for ATP in autophosphorylation reactions for human PINK1 (74.6 μM) (Hertz et al., 2013). Binding studies were also performed between TcPINK1 and AMP-PNP (a non-hydrolysable ATP analog) using ITC (Figure 4.5B). The K_d for binding was found to be 80 ± 18 μM (inverse of the association constant (K) given in Figure 4.5 B). The value is very close to the K_m from the phosphorylation kinetics study, which is consistent with the K_m being a measure of the enzyme-substrate affinity. The ITC experiment also revealed the thermodynamic parameters including ΔH, ΔG (-5.5 kcal/mol) and ΔS of the binding (Figure 4.5 B). Since ΔG of binding is negative, the binding of AMP-PNP to TcPINK1 occurs spontaneously. Both ΔH (negative) and ΔS (positive) are favorable but since the magnitude of ΔH is much greater than ΔS, the binding between TcPINK1 and AMP-PNP is mostly driven by a favorable enthalpy.

4.5 Effect of PD Mutations on Ubiquitin Kinase Activity

Studies have reported the effects of PD-linked mutations in cell-based assays on Parkin recruitment and phosphorylation (Iguchi et al., 2013). However, it is not known how these mutations impact ubiquitin phosphorylation. The availability of a recombinant stable PINK1 ortholog, TcPINK1, enabled me to test these effects *in vitro*. We chose a few PD-linked mutants of PINK1 to test Ub phosphorylation, including E240K, G309D, C388R, H271Q and A537P. Reported multiple sequence alignments of PINK1 orthologs (Figure 1.3) (Woodroof et al., 2011, Cardona et al., 2011) indicate that these residues are conserved across all species from human to drosophila except A537, which is an alanine, leucine or methionine (aliphatic) in vertebrates, but lysine (basic) in insect phyla. The residue numbers for these PD sites in TcPINK1 was determined from these alignments (human numbering in parenthesis): E217 (E240K), G285 (G309D), C363 (C388R), H247 (H271Q) and K513 (A537P). These residues were then mutated to the PD residues except for C363 that was mutated to a serine. D359N (D384 in human) mutant was used as a negative control: as mentioned in chapter 1, this residue is a part of the activation loop and is necessary for coordinating the Mg^{2+} ion to perform the catalysis, and hence does not show any Ub phosphorylation (Figure 4.6 C). Figure 4.6 A and B show the positions of some of these residues in the human PINK1 kinase domain homology model (Cardona et al., 2011). In concurrence with the lack of Parkin phosphorylation in cells by E240K, G309D and H271Q mutants of PINK1 (Iguchi et al., 2013), their corresponding mutation in TcPINK1 also abrogated Ub phosphorylation compared to WT TcPINK1 (Figure 4.6 C and D). H247Q shows some phosphorylation but E217K and G285D completely abolish Ub phosphorylation. Since E217 (E240) lies close to the activation loop (Figure 4.6 A), the introduction of a lysine at that position might affect the positioning of the loop. It is also possible that the residue might be involved in forming interactions with the substrate. E240K was found as a compound heterozygote with L489P in a PD patient (Cardona et al., 2011), a mutation that would disrupt a predicted alpha-helix in the C-lobe. Thus a combination of a "structural" and "active-site" loss-of-function mutations would completely abolish PINK1 ubiquitin kinase activity and lead to PD. G285 (G309D) lies in insert 3 of the kinase domain. Since insert 3 has been modelled as unstructured in the human PINK1 model, it is hard to make

a prediction about the structural role of this residue. It might be fair to assume that it might disturb the charge distribution in its vicinity; insert 3 is rich in positively charged residues. It has been shown that the use of KTP (instead of ATP) as a substrate rescues the deleterious effect of the G309D mutation in kinase assays for human PINK1 (Hertz et al., 2013). This implies that insert 3 (and hence G309) might be important in dictating PINK1's specificity towards its nucleotide substrate. H247 (H271) lies at the boundary of insert 2 and mediates ionic interactions with E348 in a helix of the C-lobe (Figure 4.6 B). This interaction might be important in stapling the N and C lobes together or maintaining the structure of insert 2. Another potential reason for the importance of this interaction might be the fact that L347P, which is a PD-mutant as well, would distort the helix. One of the consequences of this helix distortion might be to disrupt the H271-E348 interaction. Both and L347 and E348 are conserved in between human and TcPINK1.

PINK1 is the only kinase that has cysteine residues located at positions at the +1 and +2 positions with respect to the DFG motif in the activation loop. Studies indicate the identity of residues at the DFG+1 position are important for determining the specificity of kinases towards acceptor site in substrates (Chen et al., 2014). Moreover, C388R (DFG+2) in human PINK1 is a PD-linked mutant. To test the functional importance of thiol groups in cysteines at these positions for Ub phosphorylation, they were mutated to serines (structural analogs). However, as the results (Figure 4.D C and D) show, both single and double mutants (C362S, C363S and C362-3S) do not affect Ub phosphorylation. While it seems that these cysteine residues are not involved in ubiquitin phosphorylation reaction per se, they may play other roles in the regulation of PINK1 as post-translational modification sites, and experiments with the PD-like mutation C363R have yet to be performed.

K513 (A537P) lies in the C-terminal region PINK1. The phosphorylation assay in Figure 4.6 D indicates that it phosphorylates Ub even more than WT TcPINK1 (slightly). Secondary structure prediction indicates that this residue lies in a conserved helical region) that in this case might get disrupted and cause structural changes in the C-terminal region (Sim et al., 2012). Reports have shown that the C-terminal region might down-regulate PINK1's kinase activity (Sim et al., 2006), which is in line with the Ub phosphorylation assay as the disruption of the C-terminal

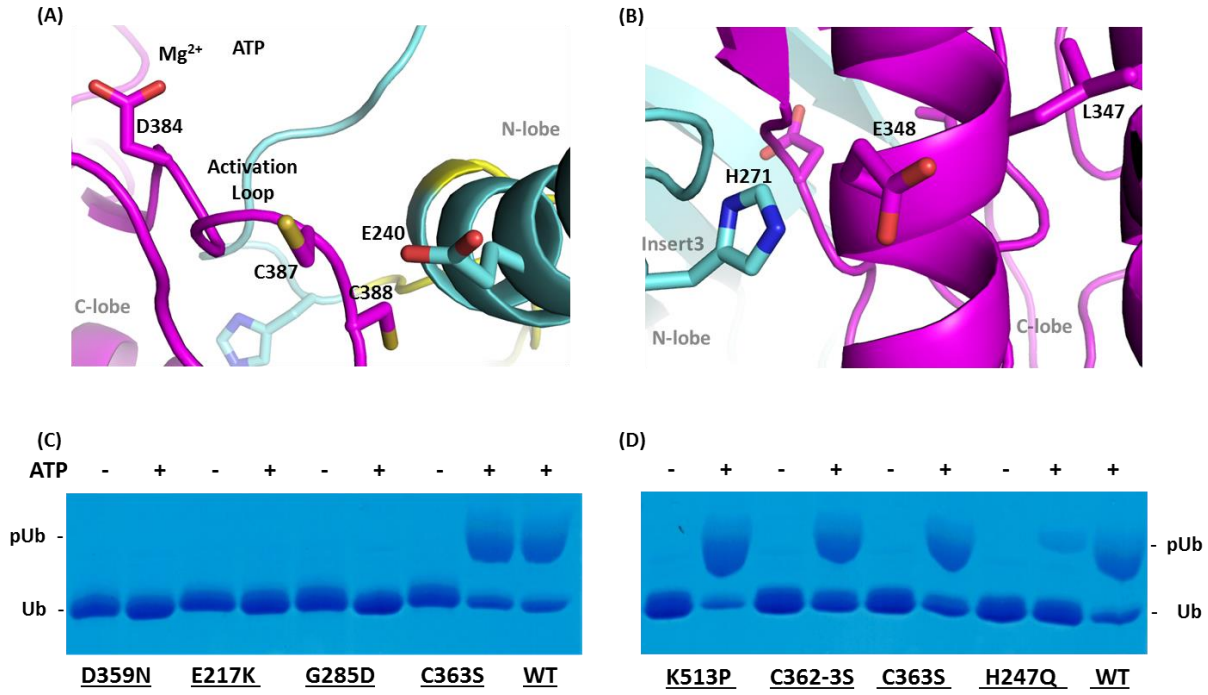

Figure 4.6 **Effect of PD mutations of PINK1 on Ub Phosphorylation** (A) and (B) showing the regions surrounding E240 and H271 respectively in the human PINK1 homology model. (C) and (D) show the His-Ub phosphorylation assays of the indicated mutants on TcPINK1 with or without ATP.

structure is leading to TcPINK1 over activation. The increase in phosphorylation remains to be quantified via kinetics. Since the C-terminal region is less conserved between human PINK1 and TcPINK1 (compared to the kinase domain), it is plausible that the C-terminal region might also serve a different role in TcPINK1.

4.6 Mapping the PINK1 binding site on Ubl

Since PINK1 is a unique kinase because of its ability to phosphorylate Parkin Ubl and Ub, it is important to understand how it recognizes these substrates. Also, as shown in section 4.4, Ubl phosphorylation is favored over Ub. Hence, what features of the Parkin Ubl makes it distinct from Ub in terms of its interaction with PINK1 is also an important question. Since the backbone ^{15}N-^{1}H amide NMR resonance assignments for the Parkin Ubl are available (Trempe et al., 2009), ^{1}H-^{15}N HSQC experiments can be performed between Ubl and proteins that interact with it to find the residues that undergo chemical shift changes. These experiments can reveal the identity of the binding site on Ubl. In order to accomplish this, a ^{1}H-^{15}N HSQC spectrum was acquired for ^{15}N-labelled Ubl and the backbone amide assignments were mapped onto the spectrum. Following that, NMR titrations were performed with starting with the

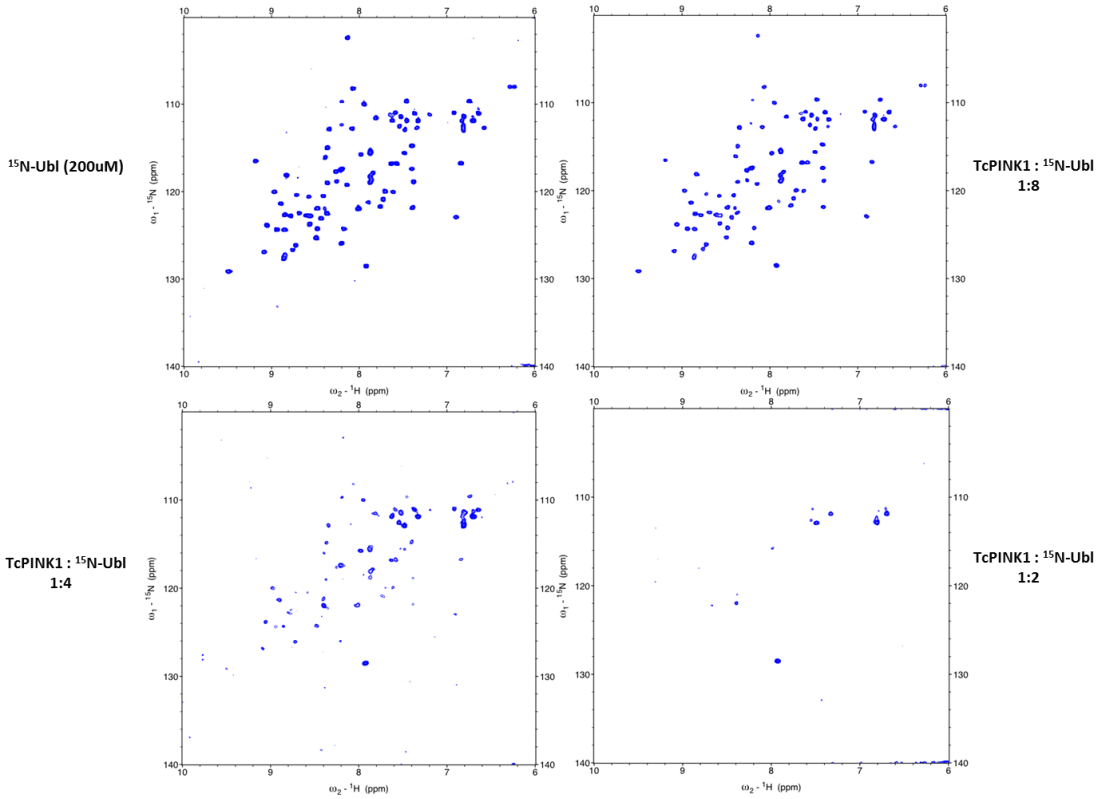

Figure 4.7 **NMR titrations show TcPINK1 and Ubl binding.** Each panel represents the addition of a different concentration of PINK1 relative to 200uM ^{15}N-Ubl.

saturating concentration (1:2) and decreasing amounts of TcPINK1 down to 1:8. ^{1}H-^{15}N HSCQ spectra were acquired for each concentration (Figure 4.7). The spectra indicate a loss of signal for ^{15}N-labelled Ubl peaks with increasing TcPINK1 which is indicative of binding between Ubl and TcPINK1; chemical shift changes in the peaks were not observed probably because of a slower-tumbling complex formed between Ubl and TcPINK1 that causes greater relaxation and line broadening. Hence the inference of interacting residues wouldn't be possible by monitoring chemical shift perturbations. In order to salvage meaningful results out of this titration experiment, we decided to calculate the signal ratio (for all peaks) between the earliest titration point (1:8) and the control spectrum Ubl spectrum without TcPINK1. The earliest titration point is also a decent choice for this purpose because the TcPINK1 concentration (25 μM) lies closest to the K_d for TcPINK1 and Ubl binding (assuming that $K_d \sim K_m$). The peaks with the smallest values for the ratios are those that disappear the fastest and potentially correspond to residues that might be interacting with TcPINK1. An arbitrary signal ratio < 0.4 was chosen as the lower cut off value. Residues fulfilling this criterion are labelled on the

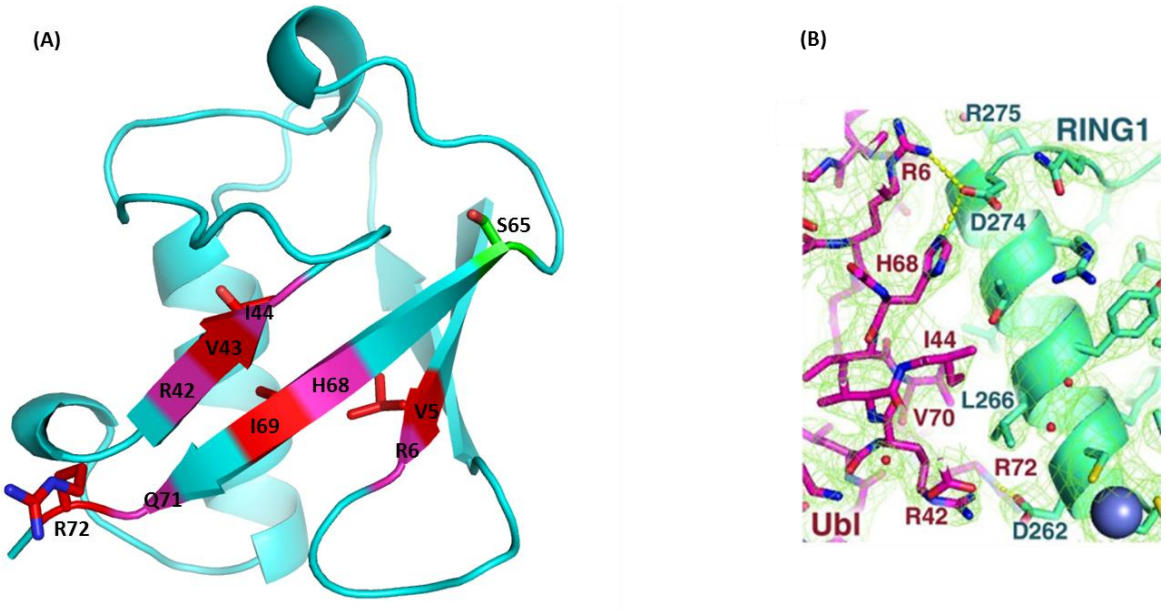

Figure 4.8 **Ubl Interaction with PINK1 and Parkin RING1** (A) (red) Residues that show the fastest loss of signal in the NMR experiment with TcPINK1, (pink) residues adjacent to them and (green) Ser65 phosphorylation site, mapped on the Ubl structure taken from PDB: 4ZYN (Sauve et al., 2015). (B) Interaction interface between Ubl and RING1 in the Parkin structure (Figure copied from (Sauve et al., 2015)).

structure of Ubl (Figure 4.8 A). Val5, Val43 and Ile69 are hydrophobic residues with their side chains pointing in towards the core, but their backbone amides (detected by NMR) are located halfway between Phe4, Arg42 and His68, which are solvent exposed. Arg72 also appears to be involved in the interaction with TcPINK1. The fact that NMR signal comes from the amide bond implies that the adjacent residues in the sequence of Ubl make the contribution towards the interaction with TcPINK1.

The interaction of Ubl with Parkin RING1 in the auto-inhibited state of Parkin is well understood owing to the availability of high-resolution crystal structures containing the Ubl domain (Sauve et al., 2015, Kumar et al., 2015). According the structures, Ubl interacts with RING1 (helix 1) via a series of hydrophobic and ionic interactions (Figure 4.8 (B); taken from (Sauve et al., 2015)). The key hydrophobic interaction are mediated by Ile44 and Val70, which interact with L266 from RING1. Ile44 and Val70 is conserved in Ub, and interactions with many Ub-binding domains are known to be mediated via these residues (Dikic et al., 2009). Since the NMR titration show Val43 signal loss, it implies that adjacent residues including Ile44 and Arg42 might be important for binding with PINK1 as well. Similarly, important ionic interactions are mediated via Arg6 and His68 which interaction with Asp274 on RING1, and Arg72 which

interacts with Asp262. Since Arg72, Ile69 and Val5 were indicated by the NMR results, it implies that His68, Arg6 and Arg72 might be important for interacting with PINK1. Hence the NMR results allude to a similarity between the interactions of Ubl with PINK1 and Parkin RING1, even though there is no homology between the two proteins. This site centered around Ile44 is also important for the binding of Parkin Ubl to the SH3 domain of Endophilin-A1 (Trempe et al., 2009). K48 has also been shown to mediate an interaction with the Endophilin-A1 SH3 domain.

In order confirm the findings from the NMR experiment, a series of Ubl mutants were generated and their phosphorylation by TcPINK1 was tested. Figure 4.9 shows the results in the form of phos-tag gels and the corresponding quantitative comparisons on bar graphs. Compared to WT Ubl, most mutants show a decrease in phosphorylation with the greatest decrease occurring for I44A, R42E and R72A (more than 3 times compared to WT), followed by H68A and R6A (more than 2 times compared to WT). R42P is also a commonly known PD-linked mutation of Parkin, although this mutation has been shown to destabilize the Ubl fold (Chaugule et al., 2011). This further strengthens the idea that these residues play an important role in binding TcPINK1 as well as the Parkin RING1 domain. For reasons mentioned previously, K48A (and its adjacent E49Q) were also tested and also show impairment in phosphorylation. Besides these residues, some residues that are not conserved in Ub were tested, with the intention of deciphering the specificity factors that allow for greater Ubl phosphorylation compared to Ub. N8 in Ubl has been shown to mediate important interactions with both Parkin RING1 and EndophilinA1 SH3 (Trempe et al., 2009), while L8 in Ub is also known to make important hydrophobic contacts with Ub-binding domains (Dikic et al., 2009). Ile 66 (adjacent to the phosphorylation site S65) in Ubl might also dictate a difference in recognition as it is a

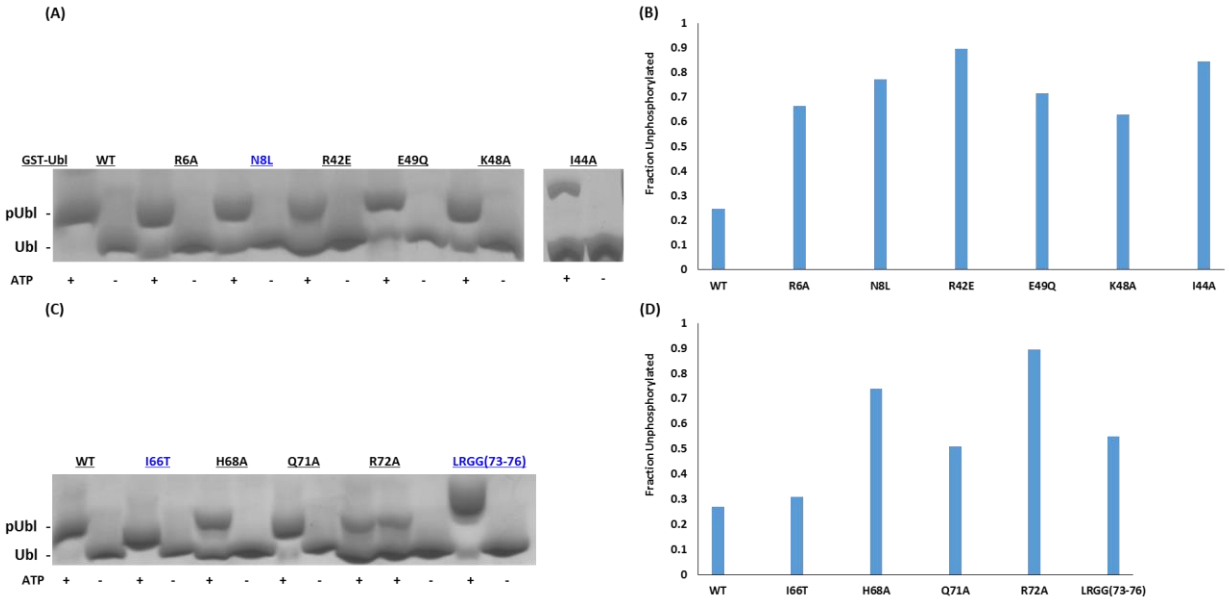

Figure 4.9 **Phosphorylation experiments between mutant forms of Ubl and TcPINK1** (A) and (C) 5mins phosphorylation experiments of mutant forms of GST-Ubl with GST-TcPINK1 (143-570). (B) and (D)Bar graphs showing the corresponding results as the ratio of remaining unphosphorylated Ubl and total Ubl (-ATP controls). Residues labelled in blue on the gel images correspond to those that were tested for investigating the specificity of Ubl for PINK1 compared to Ub.

threonine in Ub. Also the last 4 residues of Ubl PQRK are not conserved in Ub (LRGG). Hence the effect on Ubl phosphorylation was monitored by introducing the Ub residues into Ubl. Of these mutations, N8L showed the greatest decrease in phosphorylation by PINK1 (about 3 times). I66T was very similar to WT, and LRGG (73-76) showed some decrease in phosphorylation. It is important to notice that L8 in pUb forms an important contact with Parkin in the recently published structure of Parkin R0RBR in complex with pUb (Wauer et al., 2015). As opposed to this, pUbl is not known to bind strongly to Parkin R0RBR (Sauve et al., 2015). Hence the interactions that pUb makes with parkin to activate it also need to come from residues and surfaces which are distinct from pUbl. The binding of pUb to Parkin will be discussed further in the next chapter.

Future experiments would involve similar NMR experiment with Ub. It also important to perform NMR methods such TROSY experiments that can allow the chemical shifts to be mapped much more accurately for large protein complexes.

Chapter 5. Parkin activation by PINK1

Note: The results shown in this chapter (Figure 5.1, 5.2 and 5.3 A) have been published (Sauve et al., 2015) and contain contributions from other authors on the manuscript as well (as described in the acknowledgements section).

As discussed in the introduction chapter, the structure of full-length Parkin revealed an auto-inhibited structural form, because the catalytic site C431 is occluded by RING0, and the binding site for the E2 enzyme on RING1 is occluded by Ubl and the REP (Trempe et al., 2013). This implies that prior to enzymatic activation, the Ubl and REP need to be released. One possible way for that to happen could be the phosphorylation of the Ubl by PINK1 (Kondapalli et al., 2012), which could disrupt the Ubl: RING1 interaction. Molecular dynamics studies have also presented some evidence for this (Caulfield et al., 2014). Multiple studies have reported the role of pUb in the allosteric activation of Parkin in cells and *in vitro,* though both phosphorylation of Ubl and Ub were found to necessary for complete activation (Koyano et al., 2014, Kane et al., 2014, Kazlauskaite et al., 2014). What was not addressed in these studies is how Parkin interacts with pUb. This year, our group (Sauve et al., 2015), among others (Kumar et al., 2015, Kazlauskaite et al., 2015, Wauer et al., 2015), tried to answer two important questions: 1) which residues in Parkin act as the binding site for pUb? And 2) what is the precise biochemical role of pUb in terms of the activation of Parkin. The structure of Parkin (Sauve et al., 2015) revealed that sulfate ions in the crystallization conditions were bound to Parkin in 2 distinct basic residue patches: a positively charged surface formed by H302 and R305 close to the RING0-RING1 interface (Figure 5.1 A) and another positive patch formed by K161, R163 and K211. It was hypothesized that these sites could be potential pUb binding sites. Upon mutation to alanine however, only H302A (figure 5.1 C) and R305A showed a decrease in pUb binding compared to WT R0RBR of Parkin as demonstrated with ITC experiments (Figure 5.1 B); the H302A mutant alone shows about 60-fold decrease in pUb binding. SAXS data has also been used to confirm that pUb binding occurs in this region (Sauve et al., 2015). Similar findings have

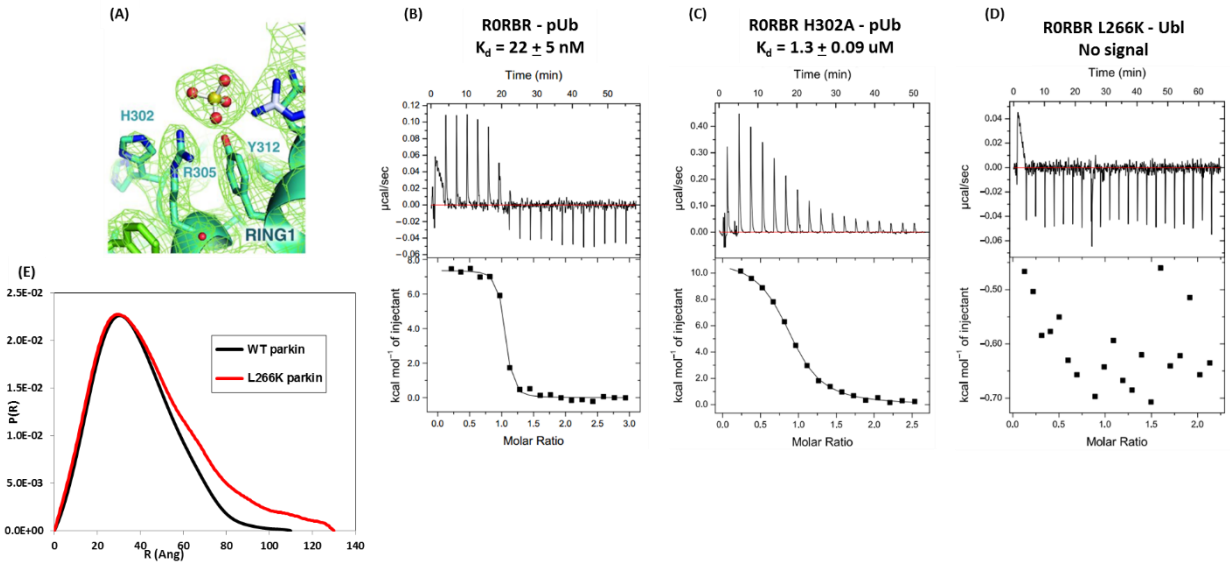

Figure 5.1 **Binding site of pUb on Parkin** (A) Sulfate ion bound at the binding interface formed by H302 and R305 (PDB: 4ZYN). ITC experiments of (B) WT R0BRB region of Parkin with pUb, (C) H302A R0RBR with pUb and (D) L266K R0RBR with Ubl. (E) P(R) curves obtained from SAXS data, comparing pairwise distance distributions of full-length Parkin WT with full-length L226K Parkin.

been reported by other groups (Kazlauskaite et al., 2015, Wauer et al., 2015, Kumar et al., 2015). As mentioned in the introduction, pUb is important for Parkin recruitment to mitochondria; H302A mutant was also found to be defective in terms of Parkin localization to mitochondria (Kazlauskaite et al., 2015).

As established in the last chapter, the PINK1 interaction surface on the Ubl, i.e. I44, H68, R72 and R6, is bound to RING1 in the auto-inhibited structure of Parkin. This implies that if PINK1 were to phosphorylate the Ubl domain, the Ubl would have to disengage from RING1 to be able to bind to PINK1, since the accessibility of PINK1 to Ser65 is limited. The affinity of the Ubl for TcPINK1 (K_m= 35 µM) established in the last chapter is slightly lesser than that of intramolecular interaction between Ubl and Parkin RING1 (~16 µM) (Sauve et al., 2015), so PINK1 is less likely to favorably bind to Ubl compared to RING1. Moreover, the Ubl is tethered to the rest of Parkin, which strongly favors the closed conformation. Hence PINK1 is not likely to phosphorylate Parkin in the auto-inhibited state. Since pUb binding to Parkin is important for its mitochondrial localization, I hypothesized that pUb was responsible for generating the conformational change necessary for PINK1 to phosphorylate Parkin. Phosphorylation assays were hence conducted on Parkin in the presence or absence of pUb using TcPINK1, and loaded on 10% Tris-Glycine gels with Phos-tag (figure 5.2 A). As visible, Parkin shows a very small

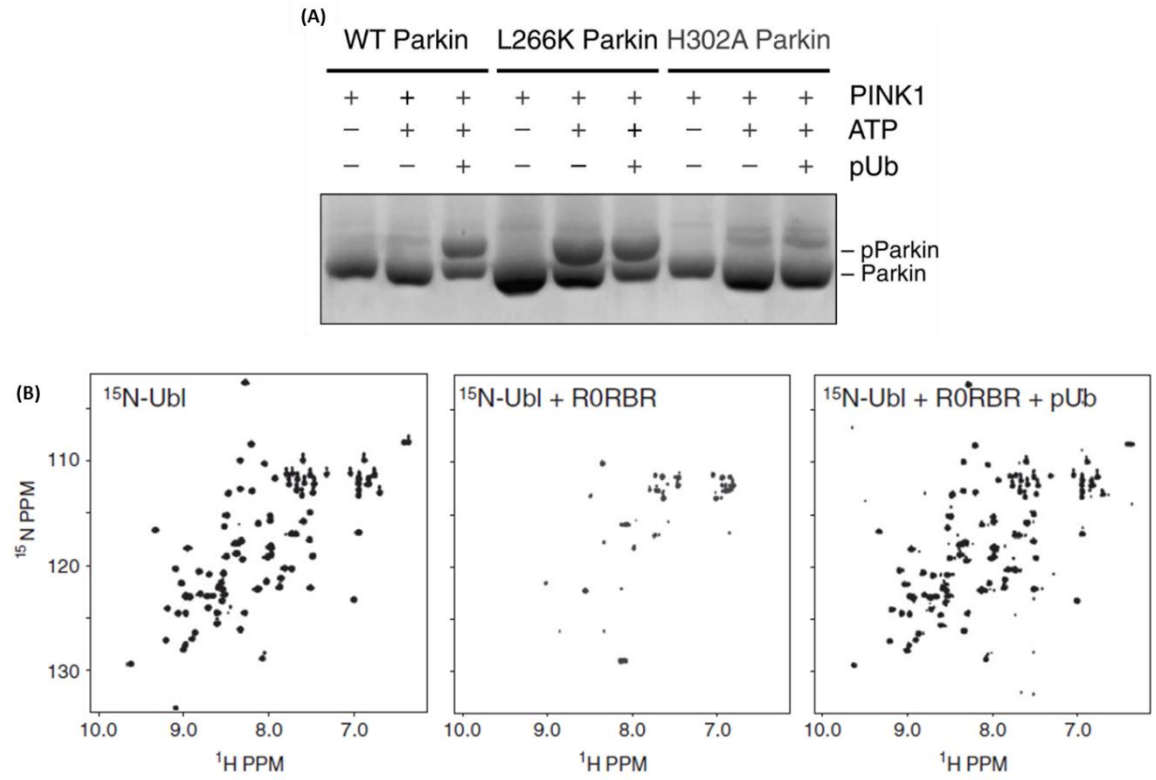

Figure 5.2 **Binding of pUb to Parkin causes Ubl release and Phosphorylation by PINK1** (A) Phos-tag gel showing a phosphorylation assay (5 minute reaction) of full-length WT, L266K and H302A Parkin with TcPINK1, in the absence or presence of equimolar quantities of pUb. (B) ^{1}H-^{15}N HSQCs of ^{15}N-Ubl (100uM) in the presence of equimolar quantities of Parkin R0RBR or Parkin R0RBR and pUb.

amount of phosphorylation in the absence of pUb in 5 mins, though nearly 50 percent of Parkin gets phosphorylated in the presence of pUb in the same time. In order to consolidate these findings, similar phosphorylation experiments were performed with the L266K mutant of Parkin. As mentioned in the previous chapter, the L266 residue on Parkin RING1 maintains hydrophobic interactions with the I44 patch on Ubl. Hence the introduction of this mutation prevents the binding of Ubl to RING1 as shown by the ITC data (Figure 5.1 D). This causes the Ubl to be repelled from the interface to produce a more open conformation or Parkin compared to WT Parkin; the SAXS paired-distance plot shows interatomic distances greater than those WT (Figure 5.1 E). The R_g calculated from SAXS for L266K (34.1 ± 0.1 Angstrom) is also significantly greater than WT (29.1 ± 0.1 Angstrom). When tested in phosphorylation assays with or without pUb, L266K showed much greater phosphorylation compared to WT even without pUb, confirming that the role of pUb is the release of the Ubl (Figure 5.2 A). No significant increase in phosphorylation was registered upon pUb addition. As expected, the

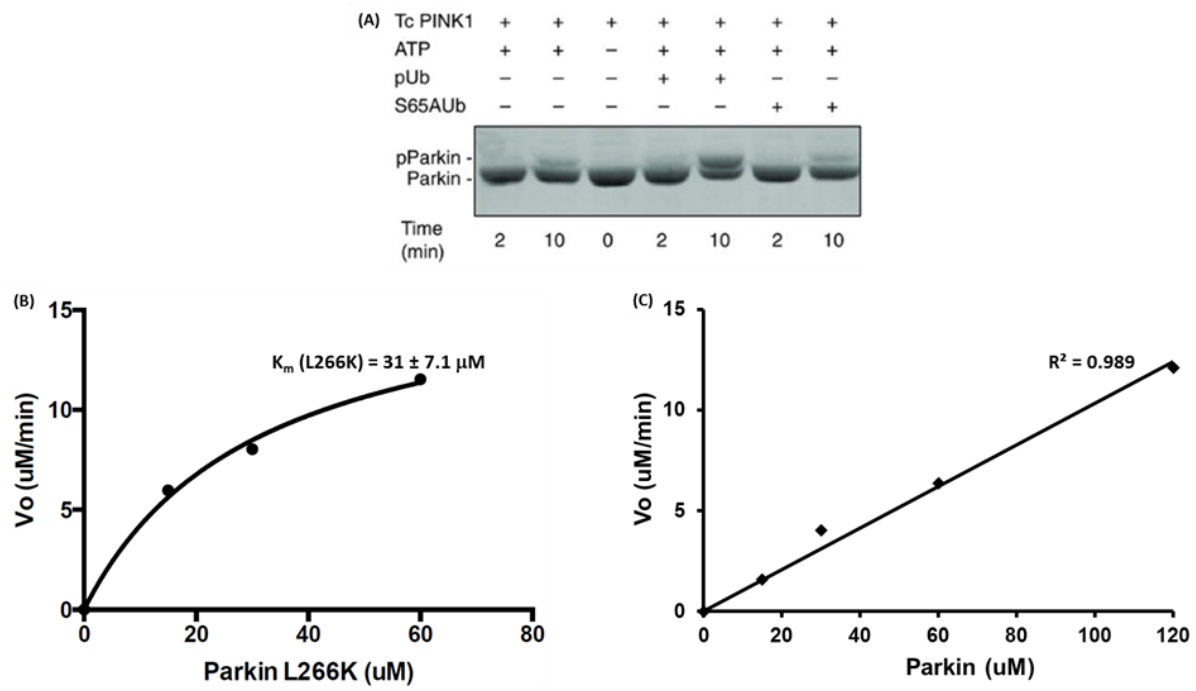

Figure 5.3 **Specificity of pUb and Kinetics of Parkin Phosphorylation** (A) Time course phosphorylation assay of Parkin by PINK1 in the presence or absence of equimolar His-pUb or His-S65A Ub. Michealis-Menten modelling of (B) L266K or (C) WT Parkin phosphorylation by TcPINK1.

H302A did not exhibit a pUb-dependent increase in phosphorylation. The phosphorylation assays were reinforced by ^{1}H-^{15}N HSQC experiments with ^{15}N-Ubl (Figure 5.2 B): the addition of R0RBR Parkin lead to a disappearance of the ^{15}N-Ubl peaks due to binding. However the signals reappeared upon the addition of pUb since Ubl is released. These observations elucidate an antagonistic relationship between pUb and Ubl binding, which explains the increase in Parkin phosphorylation upon pUb binding.

It has been shown that Parkin R0RBR can bind weakly to Ub (Sauve et al., 2015). In order to confirm that the conformational change in parkin and its increased phosphorylation was specifically due to binding of the phosphorylated form of Ub, time course Parkin phosphorylation assays were performed with or without pUb or Ub S65A. Ub S65A was used in these instead of WT because it can't get phosphorylated by PINK1 during the reaction. Figure 5.3 (A) shows the results. After 10 minutes, the reaction without pUb or the reaction with Ub S65A show only a minimal amount of phosphorylation compared to Parkin with pUb. The negligible effect of Ub S65A of Parkin phosphorylation could be because of its much weaker

binding to Parkin compared to pUb. Also, it is likely that the binding site for pUb might be distinct from Ub since the latter does not possess the negatively charged phosphate moiety needed to bind the H302 and R305 basic pocket.

Preliminary kinetic analysis was also performed on Parkin and L266K Parkin (in the same way as described in chapter 4). Since L226K mimics the effect of pUb binding to Parkin, it was chosen as model for this analysis to understand the kinetics of phosphorylation of Parkin bound to pUb. The estimated K_m for the phosphorylation of L266K parkin is very similar to that of Ubl domain alone (determined in the previous chapter). This implies Ubl is fully accessible by PINK1 for phosphorylation when Parkin it is bound to pUb. Compared to this, Parkin WT does not undergo saturation upon increase in concentration and the increase in V_0 stays linear even up to 120 μM concentration. Hence the K_m of Parkin lies beyond this concentration range. It remains to be seen if the K_m is above that of Ub to establish the preferred substrate in the absence of pUb. For either protein (WT or L266K), it is hard to concentrate the protein beyond the concentrations used in the assays, therefore the determination of K_m for WT parkin using this assay is difficult (compared to Ub). Also, the number of data point for L266K phosphorylation are limited. Nonetheless, based on this data, it is fair to conclude that the binding of pUb is a necessary step for efficient phosphorylation of Parkin by PINK1. It has also been shown that phosphorylation of Parkin is the key step for its activation; though pUb can cause increase in Parkin's E3 ligase activity as it had been previously reported (Koyano et al., 2014, Kazlauskaite et al., 2014, Kane et al., 2014), once phosphorylated Parkin (in the absence of pUb), addition of pUb causes no further increase in Parkin's activity (Sauve et al., 2015). In summary, pUb plays a role in Parkin localization to mitochondria and priming Parkin for PINK1-dependent phosphorylation.

Chapter 6. Discussion and Conclusion

PINK1 is an important neuroprotective protein and its malfunction due to genetic mutations is linked to autosomal recessive Parkinsonism. PINK1 most likely fulfills this neuroprotective role as a mitochondrial-damage sensing protein and initiates mitochondrial repair, removal and homeostasis. This thesis was inspired by the importance and roles that PINK1 plays in the cells, and aimed for its structural and functional characterization in vitro.

Chapter 3 was aimed at the discovery of PINK1 constructs that could be easily expressed in an active and soluble form in E.coli. Subsequent to expression, the purification were was optimized to improve the yield of the purified protein. We discovered that insect species including the Red red flour beetle (Tribolium castaneum), louse, ant and mountain pine beetle possess PINK1 that can be expressed in E.coli with ease and do not present problems such as low yield, instability, endogenous degradation and impurities. Additionally for TcPINK1 constructs, the kinase domain and C-terminal region both were found necessary for expression. NT was dispensable for protein expression but the length of the NT included in the construct was found to control the dimerization of protein in solution (using SEC-MALS studies). Since TcPINK1 (143-570) and (121-570) (monomer and dimer respectively) are more homogenous in solution compared to (128-570), they are better candidates for crystallization trials. The observations from both the expression tests and SEC hence guide towards making the best constructs for crystallization. Additional approaches can be used to improve protein crystallization including substitution of surface exposed hydrophobic residues (non-conserved) to hydrophilic residues to increase solubility, or amino acid substitution as a means of surface entropy reduction (replacement of flexible long chain amino acids such as lysines with short chain hydrophilic ones) to increase the chances of crystallization. Since the yield of the protein is fairly high (40 mg of protein from 1 liter), metabolic ^{13}C and ^{15}N-labelling for NMR studies is a viable option for sequential assignment of the entire construct (143-570) or using site-specific labels, of ^{13}C can be used for example for the labeling of isoleucine Cδ for methyl TROSY experiments for functional studies. While the assignment would be laborious (mutagenesis approach), it would enable functional studies in solution. This chapter is thus an important building platform of for structural

inquiries. A recent study has attempted the sequential assignment for Parkin R0RBR (~35 kDa) (Kumar et al., 2015); though TcPINK1 is bigger in size (~47kDa) the high expression levels can allow for TcPINK1 to be used for similar NMR investigations.

Chapter 4 involved functional inquires of PINK1 as a ubiquitin kinase and building up a system for kinetic studies on PINK1. The latter was accomplished by optimizing the phos-tag gel system. The V_{max} and K_m for Ub and Ubl were determined and indicated a higher affinity and catalytic efficiency of Ubl (K_m = 35 µM) phosphorylation compared to Ub (K_m = 391 uM). The cellular concentration of Ub in HEK293 cells was found to be 85 uM and even lesser in human frontal cortex and mouse brain (Kaiser et al., 2011). Since the K_m for Ub is much greater than the indicated concentrations, we hypothesize that the phosphorylation of Ub occurs on pre-ubiquinated substrates on mitochondria around PINK1, which provides PINK1 will high local concentrations of Ub. Therefore it is likely that on mitochondria PINK1 on mitochondria phosphorylates anchored ubiquitin chains (rather than free monomers). The cellular concentration of Parkin was measured is to be about 100 nM, as estimated by quantitative western blotting from mouse brain lysate (JF Trempe, personal communication) which is significantly lower than the K_m for Ubl, but in the same range as the K_d for pUb. Similarly to Ub, this Ubl phosphorylation might be possible when there is a high local concentration of Parkin due to recruitment by pUb (on mitochondria). The defects in Ub phosphorylation for some PD-linked mutants of PINK1 were also characterized in this chapter qualitatively. The list of mutants needs to be expanded, and kinetic analysis needs to be performed to indicate whether the mutations impact the affinity for substrate or the turn-over rate of phosphorylation. Based on a ^{1}H-^{15}N HSQC NMR study and subsequent phosphorylation studies, the residues on Ubl important for interacting with TcPINK1 were determined (I44, R72, H68 and R42), while some factors that promote a PINK1's specificity towards Ubl (compared to Ub) were also alluded to (N8). This was intended as a preliminary investigation for the Ubl binding site on PINK1. Other methods such as TROSY experiments can be used to elucidate the chemical shifts more clearly .To get more accurate information on the binding site and chemical shift perturbations, we could produce uniformly labeled ^{2}H,^{15}N-Ubl and ^{2}H-TcPINK1 and record a ^{1}H-^{15}N TROSY-HSQC NMR. Hydrogen-Deuterium exchange mass spectrometry can also be performed for this

purpose which can give an idea of the binding site on both PINK1 and Ubl. This method relies on figuring out regions of the protein protected from exchange due to intermolecular complex formation (Okiyoneda et al., 2013).

Chapter 5 was a part of the investigation of PINK1-dependent activation of Parkin (Sauve et al., 2015). Here we showed that the role pUb plays in activation of Parkin by binding to Parkin on its RING1 domain, and thus bringing about the conformational change that is required for PINK1 to bind to Parkin Ubl and phosphorylate it. The similarity between the kinetic parameters of phosphorylation of Ubl and L266K Parkin (representing pUb bound Parkin) suggests that the Ubl domain of Parkin is accessed by PINK1 only in the unbound form. We were unable to determine the K_m of WT Parkin alone but it is probably greater than 120 μM and we are yet to ascertain how it compares with Ub. Currently, there is debate in the field about whether phosphorylation of Ub or Parkin is the first step in the pathway following PINK1 accumulation, with opposing suggestions by different studies (Kane et al., 2014, Ordureau et al., 2014). While the phosphorylation experiment presented in this thesis suggests clearly that pUb binding is the driver of Parkin phosphorylation, there is also opposing evidence that suggests that phosphorylated Parkin binds much more strongly to pUb compared to unphosphorylated Parkin (and hence that Parkin phosphorylation needs to occur prior to its binding to pUb) (Ordureau et al., 2014, Sauve et al., 2015). Therefore, it is safe two ascertain that the two processes occur simultaneously and the unambiguous identification of the first step might not be critical to the understanding of the pathway: even a small amount of Parkin phosphorylation (at concentrations below its K_m) could potentially be sufficient to trigger its activation and build up new Ub chains which can then get phosphorylated by PINK1 to allow Parkin binding. Alternatively if Ub phosphorylation occurred first, it could bind Parkin and allow it phosphorylation and activation. In terms of Parkin activation on a molecular level, it remains to be fully understood how pUb brings about the conformational change in Parkin to release the Ubl. The Full length structure of full-length Parkin bound to pUb will be able to answer this question. Some preliminary evidence from the structure of pUb-bound louse Parkin R0RBR bound to pUb suggests that binding of pUb induces the straightening of helix 2the C-terminal helix in RING1, which might be essential to the release Ubl (Wauer et al., 2015).

On the whole, this thesis sets the ground for multiple investigations on PINK1: it documents protein expression tools necessary to yield sufficient levels of PINK1 to perform structural studies and the characterization of the novel phenomenon of Ub phosphorylation. The structure of PINK1 and understanding of Ub and Parkin binding will pave the path for structure-based drug designs to activate PINK1 in patients suffering from genetic or sporadic forms of Parkinson's disease. Since PINK1 has recently been shown to mediate initiate mitophagy even in the absence of Parkin (Lazarou et al., 2015), it should serve as an important target for therapies directed towards regulating mitochondrial quality control.

References

BARRETO, G. E., IARKOV, A. & MORAN, V. E. 2014. Beneficial effects of nicotine, cotinine and its metabolites as potential agents for Parkinson's disease. *Front Aging Neurosci,* 6**,** 340.

BEASLEY, S. A., HRISTOVA, V. A. & SHAW, G. S. 2007. Structure of the Parkin in-between-ring domain provides insights for E3-ligase dysfunction in autosomal recessive Parkinson's disease. *Proc Natl Acad Sci U S A,* 104**,** 3095-100.

BEILINA, A., VAN DER BRUG, M., AHMAD, R., KESAVAPANY, S., MILLER, D. W., PETSKO, G. A. & COOKSON, M. R. 2005. Mutations in PTEN-induced putative kinase 1 associated with recessive parkinsonism have differential effects on protein stability. *Proc Natl Acad Sci U S A,* 102**,** 5703-8.

BIR, A., SEN, O., ANAND, S., KHEMKA, V. K., BANERJEE, P., CAPPAI, R., SAHOO, A. & CHAKRABARTI, S. 2014. alpha-Synuclein-induced mitochondrial dysfunction in isolated preparation and intact cells: implications in the pathogenesis of Parkinson's disease. *J Neurochem,* 131**,** 868-77.

BRAAK, H., DEL TREDICI, K., BRATZKE, H., HAMM-CLEMENT, J., SANDMANN-KEIL, D. & RUB, U. 2002. Staging of the intracerebral inclusion body pathology associated with idiopathic Parkinson's disease (preclinical and clinical stages). *J Neurol,* 249 Suppl 3**,** III/1-5.

CARDONA, F., SANCHEZ-MUT, J. V., DOPAZO, H. & PEREZ-TUR, J. 2011. Phylogenetic and in silico structural analysis of the Parkinson disease-related kinase PINK1. *Hum Mutat,* 32**,** 369-78.

CAULFIELD, T. R., FIESEL, F. C., MOUSSAUD-LAMODIERE, E. L., DOURADO, D. F., FLORES, S. C. & SPRINGER, W. 2014. Phosphorylation by PINK1 releases the UBL domain and initializes the conformational opening of the E3 ubiquitin ligase Parkin. *PLoS Comput Biol,* 10**,** e1003935.

CHAUGULE, V. K., BURCHELL, L., BARBER, K. R., SIDHU, A., LESLIE, S. J., SHAW, G. S. & WALDEN, H. 2011. Autoregulation of Parkin activity through its ubiquitin-like domain. *EMBO J,* 30**,** 2853-67.

CHEN, C., HA, B. H., THEVENIN, A. F., LOU, H. J., ZHANG, R., YIP, K. Y., PETERSON, J. R., GERSTEIN, M., KIM, P. M., FILIPPAKOPOULOS, P., KNAPP, S., BOGGON, T. J. & TURK, B. E. 2014. Identification of a major determinant for serine-threonine kinase phosphoacceptor specificity. *Mol Cell,* 53**,** 140-7.

CHEN, Y. & DORN, G. W., 2ND 2013. PINK1-phosphorylated mitofusin 2 is a Parkin receptor for culling damaged mitochondria. *Science,* 340**,** 471-5.

CLARK, I. E., DODSON, M. W., JIANG, C., CAO, J. H., HUH, J. R., SEOL, J. H., YOO, S. J., HAY, B. A. & GUO, M. 2006. Drosophila pink1 is required for mitochondrial function and interacts genetically with parkin. *Nature,* 441**,** 1162-6.

DEAS, E., PLUN-FAVREAU, H., GANDHI, S., DESMOND, H., KJAER, S., LOH, S. H., RENTON, A. E., HARVEY, R. J., WHITWORTH, A. J., MARTINS, L. M., ABRAMOV, A. Y. & WOOD, N. W. 2011. PINK1 cleavage at position A103 by the mitochondrial protease PARL. *Hum Mol Genet,* 20**,** 867-79.

DEXTER, D. T. & JENNER, P. 2013. Parkinson disease: from pathology to molecular disease mechanisms. *Free Radic Biol Med,* 62**,** 132-44.

DIKIC, I., WAKATSUKI, S. & WALTERS, K. J. 2009. Ubiquitin-binding domains - from structures to functions. *Nat Rev Mol Cell Biol,* 10**,** 659-71.

DURCAN, T. M., KONTOGIANNEA, M., THORARINSDOTTIR, T., FALLON, L., WILLIAMS, A. J., DJARMATI, A., FANTANEANU, T., PAULSON, H. L. & FON, E. A. 2011. The Machado-Joseph disease-associated mutant form of ataxin-3 regulates parkin ubiquitination and stability. *Hum Mol Genet,* 20**,** 141-54.

FALLON, L., BELANGER, C. M., CORERA, A. T., KONTOGIANNEA, M., REGAN-KLAPISZ, E., MOREAU, F., VOORTMAN, J., HABER, M., ROULEAU, G., THORARINSDOTTIR, T., BRICE, A., VAN BERGEN EN

HENEGOUWEN, P. M. & FON, E. A. 2006. A regulated interaction with the UIM protein Eps15 implicates parkin in EGF receptor trafficking and PI(3)K-Akt signalling. *Nat Cell Biol,* 8**,** 834-42.

GEISLER, S., HOLMSTROM, K. M., SKUJAT, D., FIESEL, F. C., ROTHFUSS, O. C., KAHLE, P. J. & SPRINGER, W. 2010. PINK1/Parkin-mediated mitophagy is dependent on VDAC1 and p62/SQSTM1. *Nat Cell Biol,* 12**,** 119-31.

GONG, S., WORTH, C. L., BICKERTON, G. R., LEE, S., TANRAMLUK, D. & BLUNDELL, T. L. 2009. Structural and functional restraints in the evolution of protein families and superfamilies. *Biochem Soc Trans,* 37**,** 727-33.

GREENE, A. W., GRENIER, K., AGUILETA, M. A., MUISE, S., FARAZIFARD, R., HAQUE, M. E., MCBRIDE, H. M., PARK, D. S. & FON, E. A. 2012. Mitochondrial processing peptidase regulates PINK1 processing, import and Parkin recruitment. *EMBO Rep,* 13**,** 378-85.

GRENIER, K., MCLELLAND, G. L. & FON, E. A. 2013. Parkin- and PINK1-Dependent Mitophagy in Neurons: Will the Real Pathway Please Stand Up? *Front Neurol,* 4**,** 100.

GRIMES, D., GORDON, J., SNELGROVE, B., LIM-CARTER, I., FON, E., MARTIN, W., WIELER, M., SUCHOWERSKY, O., RAJPUT, A., LAFONTAINE, A. L., STOESSL, J., MORO, E., SCHOFFER, K., MIYASAKI, J., HOBSON, D., MAHMOUDI, M., FOX, S., POSTUMA, R., KUMAR, H., JOG, M. & CANADIAN NOUROLOGICAL SCIENCES, F. 2012. Canadian Guidelines on Parkinson's Disease. *Can J Neurol Sci,* 39**,** S1-30.

HASSON, S. A., KANE, L. A., YAMANO, K., HUANG, C. H., SLITER, D. A., BUEHLER, E., WANG, C., HEMAN-ACKAH, S. M., HESSA, T., GUHA, R., MARTIN, S. E. & YOULE, R. J. 2013. High-content genome-wide RNAi screens identify regulators of parkin upstream of mitophagy. *Nature,* 504**,** 291-5.

HEO, J. M., ORDUREAU, A., PAULO, J. A., RINEHART, J. & HARPER, J. W. 2015. The PINK1-PARKIN Mitochondrial Ubiquitylation Pathway Drives a Program of OPTN/NDP52 Recruitment and TBK1 Activation to Promote Mitophagy. *Mol Cell,* 60**,** 7-20.

HERTZ, N. T., BERTHET, A., SOS, M. L., THORN, K. S., BURLINGAME, A. L., NAKAMURA, K. & SHOKAT, K. M. 2013. A neo-substrate that amplifies catalytic activity of parkinson's-disease-related kinase PINK1. *Cell,* 154**,** 737-47.

HRISTOVA, V. A., BEASLEY, S. A., RYLETT, R. J. & SHAW, G. S. 2009. Identification of a novel Zn2+-binding domain in the autosomal recessive juvenile Parkinson-related E3 ligase parkin. *J Biol Chem,* 284**,** 14978-86.

IGUCHI, M., KUJURO, Y., OKATSU, K., KOYANO, F., KOSAKO, H., KIMURA, M., SUZUKI, N., UCHIYAMA, S., TANAKA, K. & MATSUDA, N. 2013. Parkin-catalyzed ubiquitin-ester transfer is triggered by PINK1-dependent phosphorylation. *J Biol Chem,* 288**,** 22019-32.

IMAM, S. Z., ZHOU, Q., YAMAMOTO, A., VALENTE, A. J., ALI, S. F., BAINS, M., ROBERTS, J. L., KAHLE, P. J., CLARK, R. A. & LI, S. 2011. Novel regulation of parkin function through c-Abl-mediated tyrosine phosphorylation: implications for Parkinson's disease. *J Neurosci,* 31**,** 157-63.

JIN, S. M., LAZAROU, M., WANG, C., KANE, L. A., NARENDRA, D. P. & YOULE, R. J. 2010. Mitochondrial membrane potential regulates PINK1 import and proteolytic destabilization by PARL. *J Cell Biol,* 191**,** 933-42.

JIN, S. M. & YOULE, R. J. 2013. The accumulation of misfolded proteins in the mitochondrial matrix is sensed by PINK1 to induce PARK2/Parkin-mediated mitophagy of polarized mitochondria. *Autophagy,* 9**,** 1750-7.

KAISER, S. E., RILEY, B. E., SHALER, T. A., TREVINO, R. S., BECKER, C. H., SCHULMAN, H. & KOPITO, R. R. 2011. Protein standard absolute quantification (PSAQ) method for the measurement of cellular ubiquitin pools. *Nat Methods,* 8**,** 691-6.

KANE, L. A., LAZAROU, M., FOGEL, A. I., LI, Y., YAMANO, K., SARRAF, S. A., BANERJEE, S. & YOULE, R. J. 2014. PINK1 phosphorylates ubiquitin to activate Parkin E3 ubiquitin ligase activity. *J Cell Biol,* 205**,** 143-53.

KAZLAUSKAITE, A., KONDAPALLI, C., GOURLAY, R., CAMPBELL, D. G., RITORTO, M. S., HOFMANN, K., ALESSI, D. R., KNEBEL, A., TROST, M. & MUQIT, M. M. 2014. Parkin is activated by PINK1-dependent phosphorylation of ubiquitin at Ser65. *Biochem J,* 460**,** 127-39.

KAZLAUSKAITE, A., MARTINEZ-TORRES, R. J., WILKIE, S., KUMAR, A., PELTIER, J., GONZALEZ, A., JOHNSON, C., ZHANG, J., HOPE, A. G., PEGGIE, M., TROST, M., VAN AALTEN, D. M., ALESSI, D. R., PRESCOTT, A. R., KNEBEL, A., WALDEN, H. & MUQIT, M. M. 2015. Binding to serine 65-phosphorylated ubiquitin primes Parkin for optimal PINK1-dependent phosphorylation and activation. *EMBO Rep,* 16**,** 939-54.

KITADA, T., ASAKAWA, S., HATTORI, N., MATSUMINE, H., YAMAMURA, Y., MINOSHIMA, S., YOKOCHI, M., MIZUNO, Y. & SHIMIZU, N. 1998. Mutations in the parkin gene cause autosomal recessive juvenile parkinsonism. *Nature,* 392**,** 605-8.

KONDAPALLI, C., KAZLAUSKAITE, A., ZHANG, N., WOODROOF, H. I., CAMPBELL, D. G., GOURLAY, R., BURCHELL, L., WALDEN, H., MACARTNEY, T. J., DEAK, M., KNEBEL, A., ALESSI, D. R. & MUQIT, M. M. 2012. PINK1 is activated by mitochondrial membrane potential depolarization and stimulates Parkin E3 ligase activity by phosphorylating Serine 65. *Open Biol,* 2**,** 120080.

KORNEV, A. P. & TAYLOR, S. S. 2010. Defining the conserved internal architecture of a protein kinase. *Biochim Biophys Acta,* 1804**,** 440-4.

KOYANO, F., OKATSU, K., KOSAKO, H., TAMURA, Y., GO, E., KIMURA, M., KIMURA, Y., TSUCHIYA, H., YOSHIHARA, H., HIROKAWA, T., ENDO, T., FON, E. A., TREMPE, J. F., SAEKI, Y., TANAKA, K. & MATSUDA, N. 2014. Ubiquitin is phosphorylated by PINK1 to activate parkin. *Nature,* 510**,** 162-6.

KUMAR, A., AGUIRRE, J. D., CONDOS, T. E., MARTINEZ-TORRES, R. J., CHAUGULE, V. K., TOTH, R., SUNDARAMOORTHY, R., MERCIER, P., KNEBEL, A., SPRATT, D. E., BARBER, K. R., SHAW, G. S. & WALDEN, H. 2015. Disruption of the autoinhibited state primes the E3 ligase parkin for activation and catalysis. *EMBO J,* 34**,** 2506-21.

LAI, Y. C., KONDAPALLI, C., LEHNECK, R., PROCTER, J. B., DILL, B. D., WOODROOF, H. I., GOURLAY, R., PEGGIE, M., MACARTNEY, T. J., CORTI, O., CORVOL, J. C., CAMPBELL, D. G., ITZEN, A., TROST, M. & MUQIT, M. M. 2015. Phosphoproteomic screening identifies Rab GTPases as novel downstream targets of PINK1. *EMBO J,* 34**,** 2840-61.

LANGSTON, J. W. & PALFREMAN, J. 1995a. All in the Mind. *The case of the frozen addicts*

1st ed. New York: Pantheon Books.

LANGSTON, J. W. & PALFREMAN, J. 1995b. Brain Damage. *The case of the frozen addicts*

1st ed. New York: Pantheon Books.

LANGSTON, J. W. & PALFREMAN, J. 1995c. The Forgotten Case. *The case of the frozen addicts*

1st ed. New York: Pantheon Books.

LAZAROU, M., JIN, S. M., KANE, L. A. & YOULE, R. J. 2012. Role of PINK1 binding to the TOM complex and alternate intracellular membranes in recruitment and activation of the E3 ligase Parkin. *Dev Cell,* 22**,** 320-33.

LAZAROU, M., SLITER, D. A., KANE, L. A., SARRAF, S. A., WANG, C., BURMAN, J. L., SIDERIS, D. P., FOGEL, A. I. & YOULE, R. J. 2015. The ubiquitin kinase PINK1 recruits autophagy receptors to induce mitophagy. *Nature,* 524**,** 309-14.

LIM, G. G., CHUA, D. S., BASIL, A. H., CHAN, H. Y., CHAI, C., ARUMUGAM, T. & LIM, K. L. 2015. Cytosolic PTEN-induced Putative Kinase 1 Is Stabilized by the NF-kappaB Pathway and Promotes Non-selective Mitophagy. *J Biol Chem,* 290**,** 16882-93.

LIN, M. T., CANTUTI-CASTELVETRI, I., ZHENG, K., JACKSON, K. E., TAN, Y. B., ARZBERGER, T., LEES, A. J., BETENSKY, R. A., BEAL, M. F. & SIMON, D. K. 2012. Somatic mitochondrial DNA mutations in early Parkinson and incidental Lewy body disease. *Ann Neurol,* 71**,** 850-4.

MANZANILLO, P. S., AYRES, J. S., WATSON, R. O., COLLINS, A. C., SOUZA, G., RAE, C. S., SCHNEIDER, D. S., NAKAMURA, K., SHILOH, M. U. & COX, J. S. 2013. The ubiquitin ligase parkin mediates resistance to intracellular pathogens. *Nature,* 501**,** 512-6.

MARTIN, I., DAWSON, V. L. & DAWSON, T. M. 2011. Recent advances in the genetics of Parkinson's disease. *Annu Rev Genomics Hum Genet,* 12**,** 301-25.

MCLELLAND, G. L., SOUBANNIER, V., CHEN, C. X., MCBRIDE, H. M. & FON, E. A. 2014. Parkin and PINK1 function in a vesicular trafficking pathway regulating mitochondrial quality control. *EMBO J,* 33**,** 282-95.

MORAIS, V. A., HADDAD, D., CRAESSAERTS, K., DE BOCK, P. J., SWERTS, J., VILAIN, S., AERTS, L., OVERBERGH, L., GRUNEWALD, A., SEIBLER, P., KLEIN, C., GEVAERT, K., VERSTREKEN, P. & DE STROOPER, B. 2014. PINK1 loss-of-function mutations affect mitochondrial complex I activity via NdufA10 ubiquinone uncoupling. *Science,* 344**,** 203-7.

NARENDRA, D., TANAKA, A., SUEN, D. F. & YOULE, R. J. 2008. Parkin is recruited selectively to impaired mitochondria and promotes their autophagy. *J Cell Biol,* 183**,** 795-803.

NARENDRA, D. P., JIN, S. M., TANAKA, A., SUEN, D. F., GAUTIER, C. A., SHEN, J., COOKSON, M. R. & YOULE, R. J. 2010. PINK1 is selectively stabilized on impaired mitochondria to activate Parkin. *PLoS Biol,* 8**,** e1000298.

NARENDRA, D. P., WANG, C., YOULE, R. J. & WALKER, J. E. 2013. PINK1 rendered temperature sensitive by disease-associated and engineered mutations. *Hum Mol Genet,* 22**,** 2572-89.

OKATSU, K., KIMURA, M., OKA, T., TANAKA, K. & MATSUDA, N. 2015. Unconventional PINK1 localization to the outer membrane of depolarized mitochondria drives Parkin recruitment. *J Cell Sci,* 128**,** 964-78.

OKATSU, K., OKA, T., IGUCHI, M., IMAMURA, K., KOSAKO, H., TANI, N., KIMURA, M., GO, E., KOYANO, F., FUNAYAMA, M., SHIBA-FUKUSHIMA, K., SATO, S., SHIMIZU, H., FUKUNAGA, Y., TANIGUCHI, H., KOMATSU, M., HATTORI, N., MIHARA, K., TANAKA, K. & MATSUDA, N. 2012. PINK1 autophosphorylation upon membrane potential dissipation is essential for Parkin recruitment to damaged mitochondria. *Nat Commun,* 3**,** 1016.

OKATSU, K., UNO, M., KOYANO, F., GO, E., KIMURA, M., OKA, T., TANAKA, K. & MATSUDA, N. 2013. A dimeric PINK1-containing complex on depolarized mitochondria stimulates Parkin recruitment. *J Biol Chem,* 288**,** 36372-84.

OKIYONEDA, T., VEIT, G., DEKKERS, J. F., BAGDANY, M., SOYA, N., XU, H., ROLDAN, A., VERKMAN, A. S., KURTH, M., SIMON, A., HEGEDUS, T., BEEKMAN, J. M. & LUKACS, G. L. 2013. Mechanism-based corrector combination restores DeltaF508-CFTR folding and function. *Nat Chem Biol,* 9**,** 444-54.

ORDUREAU, A., HEO, J. M., DUDA, D. M., PAULO, J. A., OLSZEWSKI, J. L., YANISHEVSKI, D., RINEHART, J., SCHULMAN, B. A. & HARPER, J. W. 2015. Defining roles of PARKIN and ubiquitin phosphorylation by PINK1 in mitochondrial quality control using a ubiquitin replacement strategy. *Proc Natl Acad Sci U S A,* 112**,** 6637-42.

ORDUREAU, A., SARRAF, S. A., DUDA, D. M., HEO, J. M., JEDRYCHOWSKI, M. P., SVIDERSKIY, V. O., OLSZEWSKI, J. L., KOERBER, J. T., XIE, T., BEAUSOLEIL, S. A., WELLS, J. A., GYGI, S. P., SCHULMAN, B. A. & HARPER, J. W. 2014. Quantitative proteomics reveal a feedforward mechanism for mitochondrial PARKIN translocation and ubiquitin chain synthesis. *Mol Cell,* 56**,** 360-75.

PACELLI, C., GIGUERE, N., BOURQUE, M. J., LEVESQUE, M., SLACK, R. S. & TRUDEAU, L. E. 2015. Elevated Mitochondrial Bioenergetics and Axonal Arborization Size Are Key Contributors to the Vulnerability of Dopamine Neurons. *Curr Biol,* 25**,** 2349-60.

PARK, J., LEE, S. B., LEE, S., KIM, Y., SONG, S., KIM, S., BAE, E., KIM, J., SHONG, M., KIM, J. M. & CHUNG, J. 2006. Mitochondrial dysfunction in Drosophila PINK1 mutants is complemented by parkin. *Nature,* 441**,** 1157-61.

PETOUKHOV, M. V., FRANKE, D., SHKUMATOV, A. V., TRIA, G., KIKHNEY, A. G., GAJDA, M., GORBA, C., MERTENS, H. D., KONAREV, P. V. & SVERGUN, D. I. 2012. New developments in the program package for small-angle scattering data analysis. *J Appl Crystallogr,* 45**,** 342-350.

POOLE, A. C., THOMAS, R. E., ANDREWS, L. A., MCBRIDE, H. M., WHITWORTH, A. J. & PALLANCK, L. J. 2008. The PINK1/Parkin pathway regulates mitochondrial morphology. *Proc Natl Acad Sci U S A,* 105**,** 1638-43.

POOLE, A. C., THOMAS, R. E., YU, S., VINCOW, E. S. & PALLANCK, L. 2010. The mitochondrial fusion-promoting factor mitofusin is a substrate of the PINK1/parkin pathway. *PLoS One,* 5**,** e10054.

PRIDGEON, J. W., OLZMANN, J. A., CHIN, L. S. & LI, L. 2007. PINK1 protects against oxidative stress by phosphorylating mitochondrial chaperone TRAP1. *PLoS Biol,* 5**,** e172.

REEVE, A., MEAGHER, M., LAX, N., SIMCOX, E., HEPPLEWHITE, P., JAROS, E. & TURNBULL, D. 2013. The impact of pathogenic mitochondrial DNA mutations on substantia nigra neurons. *J Neurosci,* 33**,** 10790-801.

RILEY, B. E., LOUGHEED, J. C., CALLAWAY, K., VELASQUEZ, M., BRECHT, E., NGUYEN, L., SHALER, T., WALKER, D., YANG, Y., REGNSTROM, K., DIEP, L., ZHANG, Z., CHIOU, S., BOVA, M., ARTIS, D. R., YAO, N., BAKER, J., YEDNOCK, T. & JOHNSTON, J. A. 2013. Structure and function of Parkin E3 ubiquitin ligase reveals aspects of RING and HECT ligases. *Nat Commun,* 4**,** 1982.

ROGOV, V., DOTSCH, V., JOHANSEN, T. & KIRKIN, V. 2014. Interactions between autophagy receptors and ubiquitin-like proteins form the molecular basis for selective autophagy. *Mol Cell,* 53**,** 167-78.

ROHMAN, M. & HARRISON-LAVOIE, K. J. 2000. Separation of copurifying GroEL from glutathione-S-transferase fusion proteins. *Protein Expr Purif,* 20**,** 45-7.

SARRAF, S. A., RAMAN, M., GUARANI-PEREIRA, V., SOWA, M. E., HUTTLIN, E. L., GYGI, S. P. & HARPER, J. W. 2013. Landscape of the PARKIN-dependent ubiquitylome in response to mitochondrial depolarization. *Nature,* 496**,** 372-6.

SAUVE, V., LILOV, A., SEIRAFI, M., VRANAS, M., RASOOL, S., KOZLOV, G., SPRULES, T., WANG, J., TREMPE, J. F. & GEHRING, K. 2015. A Ubl/ubiquitin switch in the activation of Parkin. *EMBO J,* 34**,** 2492-505.

SCHAGGER, H. 2006. Tricine-SDS-PAGE. *Nat Protoc,* 1**,** 16-22.

SCHAPIRA, A. H., COOPER, J. M., DEXTER, D., CLARK, J. B., JENNER, P. & MARSDEN, C. D. 1990. Mitochondrial complex I deficiency in Parkinson's disease. *J Neurochem,* 54**,** 823-7.

SHIBA-FUKUSHIMA, K., IMAI, Y., YOSHIDA, S., ISHIHAMA, Y., KANAO, T., SATO, S. & HATTORI, N. 2012. PINK1-mediated phosphorylation of the Parkin ubiquitin-like domain primes mitochondrial translocation of Parkin and regulates mitophagy. *Sci Rep,* 2**,** 1002.

SIAN J, Y. M., RIEDERER P 1999. MPTP-Induced Parkinsonian Syndrome. *Basic Neurochemistry: Molecular, Cellular and Medical Aspects.* 6th ed. Philadelphia: Lippincott-Raven.

SILVESTRI, L., CAPUTO, V., BELLACCHIO, E., ATORINO, L., DALLAPICCOLA, B., VALENTE, E. M. & CASARI, G. 2005. Mitochondrial import and enzymatic activity of PINK1 mutants associated to recessive parkinsonism. *Hum Mol Genet,* 14**,** 3477-92.

SIM, C. H., GABRIEL, K., MILLS, R. D., CULVENOR, J. G. & CHENG, H. C. 2012. Analysis of the regulatory and catalytic domains of PTEN-induced kinase-1 (PINK1). *Hum Mutat,* 33**,** 1408-22.

SIM, C. H., LIO, D. S., MOK, S. S., MASTERS, C. L., HILL, A. F., CULVENOR, J. G. & CHENG, H. C. 2006. C-terminal truncation and Parkinson's disease-associated mutations down-regulate the protein serine/threonine kinase activity of PTEN-induced kinase-1. *Hum Mol Genet,* 15**,** 3251-62.

SURMEIER, D. J., GUZMAN, J. N., SANCHEZ-PADILLA, J. & GOLDBERG, J. A. 2010. What causes the death of dopaminergic neurons in Parkinson's disease? *Prog Brain Res,* 183**,** 59-77.

SURMEIER, D. J., GUZMAN, J. N., SANCHEZ-PADILLA, J. & GOLDBERG, J. A. 2011. The origins of oxidant stress in Parkinson's disease and therapeutic strategies. *Antioxid Redox Signal,* 14**,** 1289-301.

TOMOO, K., MUKAI, Y., IN, Y., MIYAGAWA, H., KITAMURA, K., YAMANO, A., SHINDO, H. & ISHIDA, T. 2008. Crystal structure and molecular dynamics simulation of ubiquitin-like domain of murine parkin. *Biochim Biophys Acta,* 1784**,** 1059-67.

TREMPE, J. F., CHEN, C. X., GRENIER, K., CAMACHO, E. M., KOZLOV, G., MCPHERSON, P. S., GEHRING, K. & FON, E. A. 2009. SH3 domains from a subset of BAR proteins define a Ubl-binding domain and implicate parkin in synaptic ubiquitination. *Mol Cell,* 36**,** 1034-47.

TREMPE, J. F. & FON, E. A. 2013. Structure and Function of Parkin, PINK1, and DJ-1, the Three Musketeers of Neuroprotection. *Front Neurol,* 4**,** 38.

TREMPE, J. F., SAUVE, V., GRENIER, K., SEIRAFI, M., TANG, M. Y., MENADE, M., AL-ABDUL-WAHID, S., KRETT, J., WONG, K., KOZLOV, G., NAGAR, B., FON, E. A. & GEHRING, K. 2013. Structure of parkin reveals mechanisms for ubiquitin ligase activation. *Science,* 340**,** 1451-5.

UNOKI, M. & NAKAMURA, Y. 2001. Growth-suppressive effects of BPOZ and EGR2, two genes involved in the PTEN signaling pathway. *Oncogene,* 20**,** 4457-65.

VALENTE, E. M., ABOU-SLEIMAN, P. M., CAPUTO, V., MUQIT, M. M., HARVEY, K., GISPERT, S., ALI, Z., DEL TURCO, D., BENTIVOGLIO, A. R., HEALY, D. G., ALBANESE, A., NUSSBAUM, R., GONZALEZ-MALDONADO, R., DELLER, T., SALVI, S., CORTELLI, P., GILKS, W. P., LATCHMAN, D. S., HARVEY, R. J., DALLAPICCOLA, B., AUBURGER, G. & WOOD, N. W. 2004. Hereditary early-onset Parkinson's disease caused by mutations in PINK1. *Science,* 304**,** 1158-60.

VALENTE, E. M., BENTIVOGLIO, A. R., DIXON, P. H., FERRARIS, A., IALONGO, T., FRONTALI, M., ALBANESE, A. & WOOD, N. W. 2001. Localization of a novel locus for autosomal recessive early-onset parkinsonism, PARK6, on human chromosome 1p35-p36. *Am J Hum Genet,* 68**,** 895-900.

WANG, C., KO, H. S., THOMAS, B., TSANG, F., CHEW, K. C., TAY, S. P., HO, M. W., LIM, T. M., SOONG, T. W., PLETNIKOVA, O., TRONCOSO, J., DAWSON, V. L., DAWSON, T. M. & LIM, K. L. 2005. Stress-induced alterations in parkin solubility promote parkin aggregation and compromise parkin's protective function. *Hum Mol Genet,* 14**,** 3885-97.

WANG, X., WINTER, D., ASHRAFI, G., SCHLEHE, J., WONG, Y. L., SELKOE, D., RICE, S., STEEN, J., LAVOIE, M. J. & SCHWARZ, T. L. 2011. PINK1 and Parkin target Miro for phosphorylation and degradation to arrest mitochondrial motility. *Cell,* 147**,** 893-906.

WAUER, T. & KOMANDER, D. 2013. Structure of the human Parkin ligase domain in an autoinhibited state. *EMBO J,* 32**,** 2099-112.

WAUER, T., SIMICEK, M., SCHUBERT, A. & KOMANDER, D. 2015. Mechanism of phospho-ubiquitin-induced PARKIN activation. *Nature,* 524**,** 370-4.

WENZEL, D. M., LISSOUNOV, A., BRZOVIC, P. S. & KLEVIT, R. E. 2011. UBCH7 reactivity profile reveals parkin and HHARI to be RING/HECT hybrids. *Nature,* 474**,** 105-8.

WOODROOF, H. I., POGSON, J. H., BEGLEY, M., CANTLEY, L. C., DEAK, M., CAMPBELL, D. G., VAN AALTEN, D. M., WHITWORTH, A. J., ALESSI, D. R. & MUQIT, M. M. 2011. Discovery of catalytically active orthologues of the Parkinson's disease kinase PINK1: analysis of substrate specificity and impact of mutations. *Open Biol,* 1**,** 110012.

YAMANO, K. & YOULE, R. J. 2013. PINK1 is degraded through the N-end rule pathway. *Autophagy,* 9**,** 1758-69.

ZHANG, C., LEE, S., PENG, Y., BUNKER, E., GIAIME, E., SHEN, J., ZHOU, Z. & LIU, X. 2014. PINK1 triggers autocatalytic activation of Parkin to specify cell fate decisions. *Curr Biol,* 24**,** 1854-65.

ZHOU, C., HUANG, Y., SHAO, Y., MAY, J., PROU, D., PERIER, C., DAUER, W., SCHON, E. A. & PRZEDBORSKI, S. 2008. The kinase domain of mitochondrial PINK1 faces the cytoplasm. *Proc Natl Acad Sci U S A,* 105**,** 12022-7.